James K. Rilling
Department of Anthropology and Yerkes Regional Primate Research Center, Emory University, Atlanta, GA 30322, U.S.A.
E-mail: jrillin@emory.edu

Thomas R. Insel
Department of Psychiatry and Behavioral Sciences and Yerkes Research Center, Emory University, Atlanta, GA 30322, U.S.A.

Received 17 September 1998
Revision received 11 March 1999
and accepted 19 March 1999

Keywords: brain evolution, allometry, neocortex, anthropoids, gyrification, human.

The primate neocortex in comparative perspective using magnetic resonance imaging

In this study we use neuroanatomic data from living anthropoid primate subjects to test the following three hypotheses: (1) that the human neocortex is significantly larger than expected for a primate of our brain size, (2) that the human prefrontal cortex is significantly more convoluted than expected for our brain size, and (3) that increases in cerebral white matter volume outpace increases in neocortical gray matter volume among anthropoid primates. Whole brain MRI scans were obtained from 44 living primate subjects from 11 different species. Image analysis software was used to calculate total brain volume, neocortical gray matter volume, cerebral white matter volume, and the cross sectional area of the spinal cord in each scan. Allometric regression analyses were used to compare the relative size of these brain structures across species, with an emphasis on determining whether human brain proportions correspond with predictions based on nonhuman primate allometric trajectories. All three hypotheses were supported by our analysis. The results of this study provide additional insights into human brain evolution beyond the important observation that brain volume approximately tripled in the hominid lineage by demonstrating that the neocortex was uniquely modified throughout hominid evolution. These modifications may constitute part of the neurobiological substrate that supports some of our species most distinctive cognitive abilities.

Journal of Human Evolution (1999) **37,** 191–223
Article No. jhev.1999.0313
Available online at http://www.idealibrary.com on IDEAL

Introduction

Only two sources of evidence are available with respect to primate brain evolution (Radinsky, 1972). First, paleontological data from fossil skulls and endocasts reveal how total brain volume changed in various lineages throughout primate evolution (Tobias, 1971, 1995; Holloway, 1973, 1995). Although some cerebral sulci (e.g., the lunate sulcus) leave impressions on the surface of fossilized skulls and endocasts so that their position can be tracked across evolutionary time (Falk, 1980; Holloway & Shapiro, 1992), the study of endocasts is, at best, an estimate of brain surface anatomy without access to deep structures. The second source of data with respect to primate brain evolution comes from the comparative neuroanatomic study of extant primates (Bonin, 1941*a*, 1963; Passingham, 1973, 1982). Although this is an indirect form of phylogenetic evidence, it is an abundant source of data that permits investigation of how the internal anatomy of the brain has or has not been modified throughout primate evolution.

Comparative neuroanatomic data have been used to make inferences with respect to the evolution of the primate neocortex. Anthropoid primates typically have larger neocortices for their body size than prosimian primates (Stephan & Andy, 1969). This is not unexpected since anthropoids also have larger relative brain sizes than prosimians (Stephan & Andy, 1969; Armstrong,

0047–2484/99/080191+33$30.00/0

1985). However, anthropoids also have more neocortex for their brain size than prosimians (Radinsky, 1975; Barton, 1996). This important observation suggests that some time after the anthropoid primates diverged from prosimians (approximately 50 Ma ago), the internal proportions of the anthropoid brain were modified so that the neocortex came to occupy a larger proportion of the total volume.

With respect to the human neocortex, it is 2·9 times larger than expected for an anthropoid primate of the same body size (Passingham, 1973). Again, this is not unexpected in view of the fact that the human brain as a whole is 3·1 times larger than expected for a nonhuman anthropoid of the same body weight (Falk, 1980). When neocortical volume is regressed on total brain volume, humans do not depart from the nonhuman primate regression line (Passingham & Ettlinger, 1974). Thus, humans do not have more neocortex than expected for a primate of the same brain size. However, it has been argued (Deacon, 1988) that these analyses are biased against detecting evidence of brain reorganization in humans because one variable in the analysis (the neocortex) constitutes between 58·9% and 80·4% of the variable it is plotted against (brain weight or brain volume). When the data are reanalyzed by regressing neocortical volume on other brain structures that are distinct from the neocortex, it is found that the human neocortex is much larger than expected for a nonhuman anthropoid with the same size diencephalon or striatum (Deacon, 1988). These analyses suggest that humans uniquely depart from nonhuman primate allometric trends. However, the statistical significance of this human departure from allometry could not be evaluated because the human point was based on data from a single subject.

Other characteristics of the neocortex, besides overall volume, have also been compared across primate species. For example, the degree of cortical folding has been compared across several primate species (Zilles *et al.*, 1988, 1989). These comparisons reveal that larger primate brains are more convoluted than smaller ones, but that cortical folding increases more rapidly with brain size among anthropoid primates compared with prosimians. The regional pattern of gyrification across the brain has also been compared in several species (Zilles *et al.*, 1988, 1989). The largest discrepancy between pongid and human gyrification is in the prefrontal cortex, where the human brain appears to be uniquely gyrified.

Most of the above studies are based on analysis of the post-mortem data set of Stephan and colleagues (1970, 1981). These data suffer from several limitations. First, structure volumes obtained from fixed tissue are corrected for the shrinkage that accompanies fixation using a method that assumes gray and white matter shrink uniformly. This assumption has subsequently been disproved (Kretschmann *et al.*, 1982). Second, only two of the four great ape species are represented in the sample. Third, for the species that are represented, data are typically derived from only one or two brains so that the statistical significance of species' departures from allometry cannot be investigated. Fourth, since post-mortem brain specimens must be acquired from animals that are sacrificed or that die of natural causes, their anatomy may reflect the impact of old age or illness. Fifth, once brains are sliced in one plane of section, they cannot be resliced in another plane in order to measure a different brain structure more accurately.

In this paper we present results from the first comparative study to utilize a noninvasive imaging technology (magnetic resonance imaging—MRI) to obtain images of the brains of anthropoid primates. This study improves upon post-mortem comparative studies in the following ways: (1) structure volumes do not need to be corrected for fixation; (2) data from all four of

the great ape subjects are included; (3) multiple representatives from each species (between two and six) are included in an effort to provide an estimate of within species variance and to facilitate tests of statistical significance; (4) data are acquired from living, healthy, nonelderly adult subjects; (5) data can be sliced multiple times in any desired plane of section.

We use these new data to address some old questions in the field. For example, is the human neocortex the size that would be expected in a (hypothetical) nonhuman anthropoid primate of the same brain size? Based on Deacon's (1990) analysis of the Stephan post-mortem data set, we hypothesize that the human neocortex is significantly larger than expected for a primate of our brain size. Deacon's analysis was based on neocortical measurements that include both neocortical gray matter and the underlying cerebral white matter. Here, we conduct separate analyses for neocortical gray matter, cerebral white matter, and the combined volume of neocortical gray plus cerebral white matter. We also ask whether certain regions of the human neocortex are more or less convoluted than expected for a primate of our brain size. Based on Zilles *et al.*'s analysis of gyrification in post-mortem brains, we hypothesize that the human prefrontal cortex is significantly more gyrified than predicted for our brain size. Finally, using post-mortem data, Frahm and colleagues (1982) showed that neocortical gray matter volume does not keep pace with increases in cerebral white matter volume among primates. We hypothesize that we will find the same relationship between neocortical gray matter and cerebral white matter with our own data.

Materials and methods

Subjects

A total of 44 subjects from 11 anthropoid species received whole brain MRI scans for this study. Five anthropoid families are represented: Cebidae, Cercopithecidae, Hylobatidae, Pongidae, and Hominidae. The 11 species are: *Saimiri sciureus* (squirrel monkey), *Cebus apella* (capuchin monkey), *Cercocebus torquatus atys* (sootey mangabey), *Macaca mulatta* (rhesus macaque), *Papio cynocephalus* (baboon), *Hylobates lar* (gibbon), *Pongo pygmaeus* (orang-utan), *Gorilla gorilla* (gorilla), *Pan troglodytes* (chimpanzee), *Pan paniscus* (bonobo), and *Homo sapiens* (human). Intraspecific sample sizes range from two to six individuals. The use of multiple subjects from each species provides an estimate of intraspecies variance, usually absent in comparative studies. Adult subjects were used whenever possible so as to avoid any confounding effects of developmental changes in brain size. In some cases, fully adult subjects were unavailable and older subadult subjects were substituted. Of the 44 subjects included in the study, five are classified as subadults based on the life history table compiled by Harvey and colleagues (1987). These are an 8 year-old male gorilla, an 8 year-old male bonobo, an 8 year-old female chimpanzee, a 9 year-old male orang-utan, and a 6·5 year-old female gibbon. Because brain development typically precedes reproductive development (Tanner, 1990), these subjects' brains were probably adult-sized or nearly adult-sized. Informed consent was obtained from human subjects after the nature and possible consequences of the study were explained (HIC protocol 760-94). Nonhuman primate care was in accordance with Emory University IACUC guidelines (IACUC protocol 062-95Y).

MRI scans

Prior to scanning, nonhuman primates were anesthetized with Ketamine (10 mg/kg) and then weighed. Throughout the scan, nonhuman primates received a continuous IV infusion of propofol (10–20 mg/kg/h) for anesthesia. T1-weighted images of the entire

brain were acquired with a 1·5 Tesla Philips NT scanner (Philips Medical Systems, The Netherlands) using a gradient echo protocol with the following parameters: slice thickness = 1·2 mm, slice interval = 0·6 mm, TR = 19·0 ms, TE = 8·5 ms, field of view = 180 mm, number of signals averaged = 8, matrix = 256 × 256 pixels. Estimated spatial resolution was 0·70 mm^2. Monkeys were scanned in a prone position using the human knee coil, whereas apes were scanned in a supine position using the human head coil. Scan duration was a function of brain size. Approximate scanning time for monkeys, apes, and humans was 40 min, 60 min, and 80 min, respectively.

Measurements

All measurements were made with *Easyvision*, an image analysis software program (Philips Medical Systems, The Netherlands).

Whole brain volume. In each two-dimensional axial slice, brain tissue is identified and separated from surrounding tissues (cerebrospinal fluid, meninges, blood vessels, muscle, fat and bone) through a combination of computerized thresholding based on pixel signal intensities and manual editing. In each slice, the area of the selected tissue is calculated and these areas are integrated across all slices to arrive at a total brain volume estimate. The mean coefficients of variation (CVs) for repeated brain volume estimates were 1·6% (intra-rater) and 1·7% (inter-rater; $n = 8$).

Neocortical gray matter volume. An MRI image is a map of pixels of different signal intensities. Pixels in gray matter have lower signal intensities than those in white matter. The software program can be instructed to include pixels that lie within a defined range of signal intensities. In principle, therefore, it should be easy to separate white matter from gray matter using automated procedures. Unfortunately, however, most MRI scans possess gradients in signal intensity, so that the signal intensity of gray matter pixels in one part of an image differs from that in another part of the image. Thus, a single threshold cannot be specified that is appropriate for an entire slice. For this reason, our neocortical gray matter volume estimates are based on manual tracing.

The method we adopted is as follows. Each brain was divided into five stacks of images, each with an equal number of slices. The number of slices in each stack was a function of brain size. Cortical gray matter was manually traced in the middle slice of each of the five stacks. A gray matter threshold was then selected in the same slice and adjusted until the area it highlighted approximated that obtained by manual tracing (in five slices through a mangabey brain, this approximation differed from the manually traced area by an average of 1·0%). Although the highlighted area did not exactly correspond to the gray matter area for the whole slice (because of the signal intensity gradient), it seemed to be a reasonable compromise of the setting that would be best in the anterior and posterior portion of the slice. The gray matter threshold for this slice was then automatically applied to all other slices in the same stack of images. The threshold was then reestablished in the middle slice from the next stack of images. This procedure allowed adjustments to be made for the gradient in signal intensity from the top to the bottom of the brain (i.e., across the slices in a stack of axial images), in addition to those within slices. The thresholding procedure highlights all gray matter in an MRI slice. To obtain an estimate of the volume of neocortical gray matter, subcortical gray matter must be edited out of each slice in which it appears. The basal ganglia (i.e., the caudate nucleus, the putamen, and globus pallidus), the

amygdala, and the hippocampus were all excluded from the neocortex.

Intra-rater reliability of neocortical volume estimates was assessed by repeating measurements on six of the 44 brains. The mean coefficient of variation for repeated neocortical volume estimates was 1·4%. The main source of measurement error in the method lies in the perception of gray–white boundaries when tracing manually. To provide an estimate of inter-rater reliability, one of the authors and a second rater traced cortical gray matter areas in ten axial slices (two slices from each of five different brains). The mean percentage coefficient of variation for repeated cortical gray matter areas was 4·3%.

To check the accuracy of our method, we compared our neocortical volumes with those obtained by manually tracing a more complete sample of slices. We manually traced the area of the neocortex in both hemispheres of a human brain (total brain volume = 1426·0 cc) and a capuchin monkey brain (total brain volume = 77·3 cc). In the human brain we traced 23 horizontal sections spaced 5·0 mm apart, and in the capuchin brain we traced 22 horizontal sections spaced 1·0 mm apart. The results are given in the following table.

Species	Manual tracing (cc)	Our method (cc)	% difference
Human	639	615·2	3·7
Capuchin	39·3	38·2	2·8

These results show that the neocortical volumes obtained using our method very closely approximate those obtained with manual tracing.

Cerebral white matter volume. Brains were oriented in the plane of the anterior and posterior commissures and then sliced into ten evenly spaced coronal sections. In the left hemisphere of each slice, the area of the cerebral white matter was traced manually (see Figure 1). After measuring all ten slices, the areas were summed and multiplied by the distance between slices to yield an estimate of the cerebral white matter volume for the left hemisphere. Left hemisphere values were doubled to approximate whole brain values. Cerebral white matter volume measurements excluded the internal capsule. Intra-rater reliability was estimated by repeating measurements of cerebral white matter area on a sample of ten coronal slices, two from each of five different subjects. The mean coefficient of variation for repeated cerebral white matter areas was 2·32%.

Cross-sectional area of the spinal cord. All scans were reformatted to obtain a true mid-sagittal section. In this image, the dorsal surface of the medulla forms a straight line. The cross-sectional area of the spinal cord was measured in a slice perpendicular to this line at the junction between the medulla and the spinal cord. The junction could be identified as the point where the ventral bulge of the medulla (representing the pyramids) terminated caudally. Intra-rater reliability was estimated by repeating spinal cord area measurements in seven brains. The mean coefficient of variation for repeated spinal cord area measures was 7·1%.

Gyrification index. The gyrification index (GI) is a measure of cortical folding developed by Zilles and colleagues (1988, 1989). We applied this method to our own data as follows: all brains were oriented in the plane of the anterior and posterior commissures and then sliced into ten evenly spaced coronal sections. The first coronal slice was 1/11 the distance from the anterior to the posterior pole of the brain, the second was 2/11, etc. In the left hemisphere of each slice, both the length of the total neocortical surface

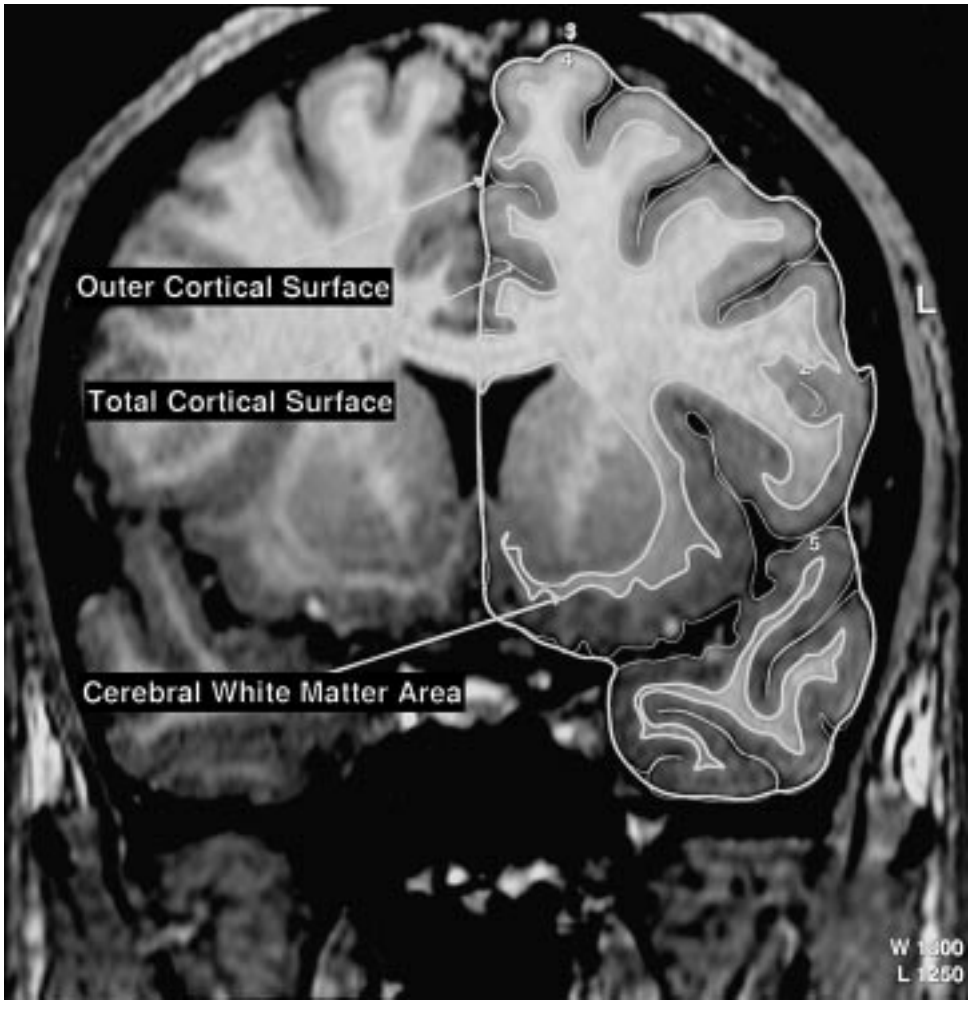

Figure 1. Method for measuring gyrification indices and cerebral white matter volumes. Three different tracings were made in the left hemisphere of ten coronal slices throughout each brain in order to measure the length of the outer cortical surface, the length of the total cortical surface (including cortex buried within cerebral sulci), and the area of the cerebral white matter. Gyrification indices were calculated as the ratio of the length of the total cortical surface to the length of the outer cortical surface. Cerebral white matter volume was calculated by summing areas across all ten slices and multiplying by the slice thickness.

(including cortex buried within sulci) and the length of the superficially exposed cortex were measured (see Figure 1). The gyrification index is the ratio of the total neocortical length to the superficially exposed neocortical length. Thus, a completely smooth cortex would have a GI of 1, and larger values reflect greater convolutedness. The hippocampus was excluded, but cortical islands within white matter that had been separated from the superficially exposed cortex because of tangential sectioning were included. In measuring the superficially exposed cortex, the opening of a sulcus was closed by a line from the top of a gyrus to the top or crown of the adjoining one.

Accuracy. The accuracy of MRI measures was assessed by comparing them with post-mortem measures from a single rhesus macaque that was scanned just prior to being sacrificed for clinical reasons. The fresh, post-mortem brain was sliced in the coronal plane and digitized images of eight slices were captured and imported to NIH Image. By reformatting the MRI scans, images were obtained that looked nearly identical to the post-mortem images in terms of their pattern of gyrification. Cortical gray matter area was manually traced in the matching slices from both sets of images and values were compared. The correlation coefficient between the MRI and post-mortem gray matter areas was 0·91 (n=8). The coefficient of variation between matching MRI and post-mortem measures was 2·6 ± 0·4% (mean ± S.E.). On average, MRI measures underestimated post-mortem measures by 0·25%, but with substantial variance (range: − 8·2%, 9·7%; S.E.=2·0%).

Statistical analyses

Statistical analyses were performed using *Systat* (version 5 for the Macintosh). Allometric relationships between variables were investigated by fitting least-squares regression lines through bivariate logarithmic plots. Logarithmic plots make the data easier to see and tend to equalize the variance in the dependent variable across different values of the independent variable, an assumption for regression analyses. The fundamental allometric equation is $Y=aX^b$, where Y=the size of one part of an organism, X=the size of the whole organism or the size of some other part, a=a constant and b=the scaling exponent that describes how Y changes with respect to changes in X. If $b>1$ (referred to as a positively allometric relationship when X and Y are dimensionally equivalent), increases in Y outpace increases in X. If $b<1$ (referred to as a negatively allometric relationship), increases in Y do not keep pace with increases in X. If $b=1$ (an isometric relationship), the relationship is linear, and Y and X increase at the same pace. When log-transformed, the equation becomes $\log Y=\log a+b \log X$ so that, when plotted on log co-ordinates, the function becomes a straight line with a slope equivalent to the value of the scaling exponent (b) in the power function. Thus, when log transformed, positively allometric relationships become straight lines with slopes greater than 1, negatively allometric relationships become straight lines with slopes less than 1, and isometric relationships become straight lines with slopes equal to 1. The slopes of our regression analyses will be interpreted accordingly.

Relative brain size and relative neocortical size in each species were assessed by quantifying species deviations from the best fit, least-squares regression line. Following Jerison (1973), one method of expressing relative brain size is to divide the observed brain volume by the brain volume predicted by a best-fit regression line through a plot of brain weight *vs.* body weight. These ratios express how many times larger a brain is than expected. When used to calculate relative brain size, these ratios will be referred to as encephalization ratios (ERs). When used to calculate relative neocortical size, they will be referred to as neocortical ratios (NRs). A second method of quantifying relative brain size is to subtract the expected brain volume from the observed. These differences will be referred to as encephalization differences (EDs) and express how much larger a brain is than expected. Differences between observed and expected neocortical volumes will be referred to as neocortical differences (NDs).

Other line fitting techniques such as major axis and reduced major axis regression produced nearly identical results to those obtained using least-squares regression. Consequently, only the results of the least-squares analyses are reported here.

Results

Table 1 provides the mean body weight, cross-sectional area of the spinal cord, brain volume, neocortical gray matter volume and cerebral white matter volume for each of the 11 species of anthropoid primates in our sample. Results from the analysis of relative brain size are presented below. Afterwards, we present results of the analyses used to test the three hypotheses enumerated in the introduction.

Relative brain size

To compare brain volume relative to body weight across our sample, log brain volume is plotted *vs.* log body weight in Figure 2(a). Because humans are obvious outliers in terms of relative brain size, including them in the regression would substantially alter the slope of the line and the magnitude of species' residuals. Therefore, the least-squares regression line is fit through the 10 species of nonhuman anthropoids. The slope is less than 1, indicating that the relationship is negatively allometric. Thus, increases in brain volume do not keep pace with increases in body weight across our sample. The regression line describes the expected brain volume for an average anthropoid primate of any given body weight. We assume that if the 95% confidence interval around the observed brain volume excludes the value predicted by the regression line, the observed brain volume is significantly different from the expected brain volume. Table 2 lists the (log) expected brain volume and the 95% confidence interval around the (log) observed volume for each species. The human brain is significantly larger than expected for a primate of our body size, whereas rhesus macaques have smaller brains than expected for primates of their body size.

From Figure 2(a) each species relative brain size can be quantified as described in the methods section. Encephalization ratios (ERs) and encephalization differences (EDs) are provided in Table 2. Encephalization ratios are higher among apes than monkeys, with the exception of capuchin monkeys who have the highest ER of our nonhuman sample. The picture is similar when EDs are used to quantify relative brain size, except that both bonobos and gorillas are more encephalized than capuchin monkeys.

All of the nonhuman subjects in our sample were raised in captivity, which involves reduced amounts of physical activity that can cause subjects to become overweight. Overweight subjects have larger bodies for their brain sizes and consequently appear underencephalized. To evaluate that possibility, the analysis in Figure 2(a) is repeated in Figure 2(b) using species' published body weights (Harvey *et al.*, 1987; Rowe, 1996) rather than actual body weights. Table 3 lists the expected brain volume (predicted from the regression line), the 95% C.I. around the observed brain volume, the ER and the ED for each species based on the analysis in Figure 2(b). Both humans and chimpanzees have significantly larger brains than expected for their body weight, whereas sootey mangabeys have significantly smaller brains than expected for their body weight. ERs are highest among the great apes and capuchin monkeys; although gorillas have the lowest ratio. EDs are highest among the great apes, also with the exception of gorillas. Capuchin monkeys are less encephalized than the great apes using ED, but appear more encephalized than other monkeys, gibbons, and gorillas.

Another approach to measuring relative brain size is to compare brain volume with the cross-sectional area of the spinal cord at its junction with the medulla. The latter is thought to provide an indication of the amount of incoming somatosensory and outgoing motor information a brain must process (Passingham, 1982). Thus, we

Table 1 Data on 11 species of anthropoid primates

Species	*N*	Body weight (kg)	Spinal cord area (mm^2)	Brain volume (cc)	Neocortical gray matter (cc)	Cerebral white matter (cc)
H. sapiens	3M 3F	67·7 ± 4·9	103·0 ± 1·4 (5)	1298·9 ± 52·0	583·0 ± 15·2	397·4 ± 24·6
P. paniscus	2M 2F	45·4 ± 7·8	70·9 ± 3·0	311·2 ± 11·0	142·9 ± 7·6	75·6 ± 4·7
P. troglodytes	3M 3F	55·4 ± 6·5	106·4 ± 7·0 (4)	337·3 ± 15·8	147·1 ± 7·0	90·9 ± 5·6
G. gorilla	1M 1F	61·7 ± 6·3	117·6 ± 16·6	397·3 ± 66·6	152·7 ± 31·7	94·2 ± 19·4
P. pygmaeus	3M 1F	73·5 ± 11·9	110·5 ± 16·8	406·9 ± 28·7	193·3 ± 23·5	94·4 ± 9·7
H. lar	2M 2F	5·4 ± 0·5	43·6 (1)	83·0 ± 5·6	39·9 ± 3·2 (3)	16·7 ± 1·4
P. cynocephalus	2M 0F	21·9 ± 1·3	73·4 (1)	143·3 ± 15·9	65·0 ± 11·1	35·1 ± 5·6
M. mulatta	2M 2F	10·4 ± 0·9	51·2 ± 1·2 (3)	79·1 ± 3·4	36·5 ± 2·8	19·2 ± 1·4
C. atys	2M 2F	8·8 ± 1·2	No data	98·9 ± 1·6	42·7 ± 2·7 (3)	21·2 ± 1·5
C. apella	2M 2F	3·2 ± 0·5	38·6 ± 1·9 (3)	66·5 ± 5·3	31·9 ± 3·5	13·1 ± 1·4
S. sciureus	3M 1F	0·9 ± 0·2	18·8 (1)	23·1 ± 0·8	11·7 ± 0·8	4·8 ± 0·2 (3)

Some structures could not be measured in some subjects because of inadequate image coverage or quality. When the number of subjects used to calculate the mean structure size is less than the total number of subjects for that species, the former is indicated in parentheses next to the structure size. For example, in several scans the cross-sectional area of the spinal cord could not be measured.

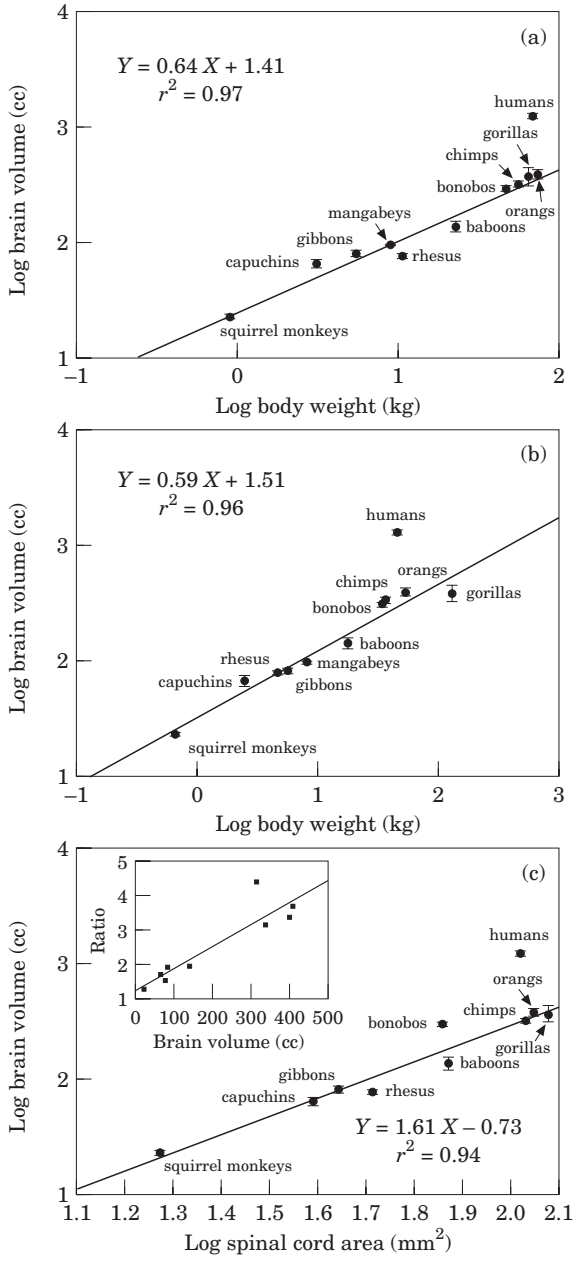

Figure 2. Relative brain size in anthropoid primates. (a) Logarithmic plot of brain volume *vs.* body weight with regression line fit through ten nonhuman primate species, using actual body weights obtained from subjects. (b) Logarithmic plot of brain volume *vs.* body weight with regression line fit through ten nonhuman primate species, using published body weight estimates. (c) Logarithmic plot of brain volume *vs.* spinal cord area with regression line fit through nine nonhuman primate species. Inset: plot of ratio of brain volume to spinal cord area *vs.* brain volume for nine nonhuman anthropoid species.

Table 2 Relative brain size in 11 anthropoid primate species, from Figure 1(a)

Species	Common name	Log obs. brain vol. with 95% C.I.	Log exp. brain vol.	ER (O/E)	ED (0 − E)
H. sapiens	Human	3·11 (3·07, 3·15)*	2·58	3·4	917
P. paniscus	Bonobo	2·49 (2·42, 2·56)	2·47	1·05	15·7
P. trolgodytes	Chimpanzee	2·53 (2·48, 2·58)	2·53	1·01	1·7
G. gorilla	Gorilla	2·60 (2·02, 3·19)	2·56	1·1	37·7
P. pygmaeus	Orang-utan	2·61 (2·51, 2·71)	2·6	1·01	4·8
H. lar	Gibbon	1·92 (1·82, 2·01)	1·88	1·1	7·4
P. cynocephalus	Baboon	2·16 (1·59, 2·73)	2·27	0·77	− 42
M. mulatta	Rhesus monkey	1·9 (1·84, 1·96)*	2·06	0·69	− 36
C. atys	Mangabey	2·0 (2·03, 1·97)	2·01	0·96	− 4·5
C. apella	Cebus	1·82 (1·71, 1·93)	1·73	1·23	12·4
S. sciureus	Squirrel monkey	1·36 (1·31, 1·41)	1·38	0·96	− 0·9

*=95% C.I. around observed brain volume excludes expected value.

Table 3 Relative brain size in 11 anthropoid primate species from Figure 1(b)

Species	Common name	Log obs. brain vol.	Log exp. brain vol.	ER (O/E)	ED (O − E)
H. sapiens	Human	3·11 (3·07, 3·15)*	2·48	4·31	997·2
P. paniscus	Bonobo	2·49 (2·42, 2·56)	2·42	1·18	47·6
P. troglodytes	Chimpanzee	2·53 (2·48, 2·58)*	2·43	1·25	67·5
G. gorilla	Gorilla	2·60 (2·02, 3·19)	2·75	0·71	− 165·3
P. pygmaeus	Orang-utan	2·61 (2·51, 2·71)	2·53	1·21	70·1
H. lar	Gibbon	1·92 (1·82, 2·01)	1·95	0·94	− 5·5
P. cynocephalus	Baboon	2·16 (1·59, 2·73)	2·24	0·82	− 31·8
M. mulatta	Rhesus monkey	1·9 (1·84, 1·96)	1·9	0·99	− 0·5
C. atys	Mangabey	2·0 (2·03, 1·97)*	2·04	0·91	− 10·3
C. apella	Cebus	1·82 (1·71, 1·93)	1·74	1·2	11·2
S. sciureus	Squirrel monkey	1·36 (1·31, 1·41)	1·41	0·91	− 2·4

*=95% C.I. around observed brain volume excludes expected value.

assume that the size of the brain in relation to spinal cord area provides an indication of the amount of neural tissue a species possesses relative to the amount of somatosensory and motor information it must process. Figure 2(c) is a logarithmic plot of brain volume *vs.* the cross-sectional area of the spinal cord, with the regression line fit through nine nonhuman species (data on spinal cord area were unavailable from mangabeys). The slope is greater than 1, indicating that increases in brain volume outpace increases in spinal cord area and the ratio of brain volume to spinal cord area predictably increases with increasing brain size [see Figure 2(c) inset]. Isometric growth predicts a slope of 1·5 for the regression of a volume on a surface area. The 95% confidence interval around the observed slope (1·24, 1·98) does not exclude 1·5. Expected brain volumes, observed brain volumes, ERs and EDs from Figure 2(c) are provided in Table 4. Both humans and bonobos have significantly larger brains than expected for their spinal cord areas, whereas rhesus monkeys have significantly

Table 4 Relative brain size in 11 anthropoid primate species from Figure 1(c)

Species	Common name	Log obs. brain vol.	Log exp. brain vol.	ER (O/E)	ED (O − E)
H. sapiens	Human	3·11 (3·07, 3·15)*	2·51	4·01	975
P. paniscus	Bonobo	2·49 (2·42, 2·56)*	2·25	1·75	134
P. troglodytes	Chimpanzee	2·53 (2·48, 2·58)	2·53	0·99	− 4·2
G. gorilla	Gorilla	2·60 (2·02, 3·19)	2·6	0·99	− 3·9
P. pygmaeus	Orang-utan	2·61 (2·51, 2·71)	2·56	1·12	44
H. lar	Gibbon	1·92 (1·82, 2·01)	1·91	1·02	1·8
P. cynocephalus	Baboon	2·16 (1·59, 2·73)	2·27	0·76	− 44·5
M. mulatta	Rhesus monkey	1·9 (1·84, 1·96)*	2·02	0·75	− 26·1
C. atys	Mangabey	2·0 (2·03, 1·97)			
C. apella	Cebus	1·82 (1·71, 1·93)	1·83	1·0	− 0·2
S. sciureus	Squirrel monkey	1·36 (1·31, 1·41)	1·32	1·1	2·1

*=95% C.I. around observed brain volume excludes expected value.

smaller brains than expected for their spinal cord area.

Neocortical gray matter volume

To compare neocortical volume relative to body weight across our sample, log neocortical volume is plotted *vs.* log body weight in Figure 3, using actual body weights. Again, humans are assumed to be outliers and a least-squares regression line is fit through the 10 nonhuman species. The regression line defines the expected neocortical volume for a typical anthropoid primate of any given body weight. The slope (0·61) is only slightly less than that for the regression of brain volume on body weight [0·64, see Figure 2(a)]. Expected neocortical volumes, observed neocortical volumes, neocortical ratios (NRs) and the neocortical differences (NDs) for each species from Figure 3 are provided in Table 5. The human neocortex is significantly larger than expected for an anthropoid primate of our body size. In addition, the rhesus macaque neocortex is sigificantly smaller than expected for a primate of its body size. In general, ape NRs are higher than monkey NRs, with the exception of capuchin monkeys, who have the largest relative neocortex size among the nonhuman species. However, as with ED, when ND values are used capuchins have a smaller relative neocortex size than some of the great ape species (bonobos and orang-utans).

To determine how the proportion of neocortex within the brain changes across our sample and to test the hypothesis that the human neocortex is larger than expected for a primate of our brain size, log neocortical volume is plotted *vs.* log brain volume in Figure 4(a). Because there is no *a priori* reason to assume that humans are outliers in this analysis, the least-squares regression line is fit through all 11 species data points. The slope is 0·98, suggesting that increases in neocortical volume nearly keep pace with increases in brain volume (the relationship is approximately isometric). However, neocortical gray matter constitutes between 38 and 51% of total brain volume in our sample. Therefore, Figure 4(a) involves the regression of a large part of a variable on itself (Deacon, 1988). To alleviate this problem, neocortical gray matter volume is plotted *vs.* the volume of the rest of the brain (brain volume–neocortical volume) in Figure 4(b). The slope of the regression line through the 11 species' data points is 0·94, suggesting that neocortical gray matter volume does not keep pace with increases in the volume of the rest of the brain. However, the 95% C.I. for the slope (0·87, 1·01) does not

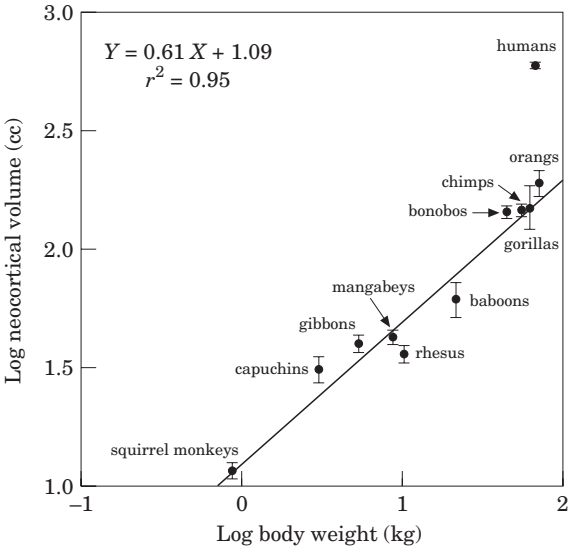

Figure 3. Relative neocortical size in anthropoid primates. Logarithmic plot of neocortical gray matter volume *vs.* body weight with regression line fit through ten nonhuman primate species, using actual body weights obtained from subjects.

Table 5 Relative neocortical size in 11 species of anthropoid primate from Figure 2

Species	Common name	Log observed neo vol. (cc)	Log expected neo vol. (cc)	NR (O/E)	ND (O − E)
H. sapiens	Human	2·77 (2·74, 2·80)*	2·21	3·6	422
P. paniscus	Bonobo	2·16 (2·09, 2·23)	2·1	1·13	16·8
P. troglodytes	Chimpanzee	2·17 (2·12, 2·22)	2·15	1·03	4·7
G. gorilla	Gorilla	2·18 (1·02, 3·34)	2·18	1·0	0·6
P. pygmaeus	Orang-utan	2·29 (2·12, 2·46)	2·23	1·14	24·1
H. lar	Gibbon	1·6 (1·49, 1·71)	1·54	1·16	5·5
P. cynocephalus	Baboon	1·81 (0·86, 2·76)	1·91	0·8	− 15·8
M. mulatta	Rhesus monkey	1·56 (1·46, 1·66)*	1·71	0·71	− 14·8
C. atys	Mangabey	1·63 (1·51, 1·75)	1·67	0·92	− 3·7
C. apella	Cebus	1·50 (1·33, 1·67)	1·4	1·28	6·9
S. sciureus	Squirrel monkey	1·07 (0·97, 1·16)	1·06	1·02	0·2

*=95% C.I. around observed brain volume excludes expected value.

exclude 1·00, so that an isometric relationship cannot be rejected. From Figure 4(b), humans are the only species with an observed neocortical volume significantly different from that expected for a primate of the same brain size. Specifically, the human neocortex is 15% (or 78 cc) larger than expected. If the data in Figure 4(b) are replotted with the regression line fit through the ten nonhuman species [Figure 4(c)], the slope decreases to 0·91 (95% C.I.=0·82, 1·00) and the human neocortex is 24% (or 115 cc) larger than predicted by the regression line. For no other species does the observed neocortical volume differ significantly from the expected. The discrepancy between the observed and expected human neocortical volume can be perceived more

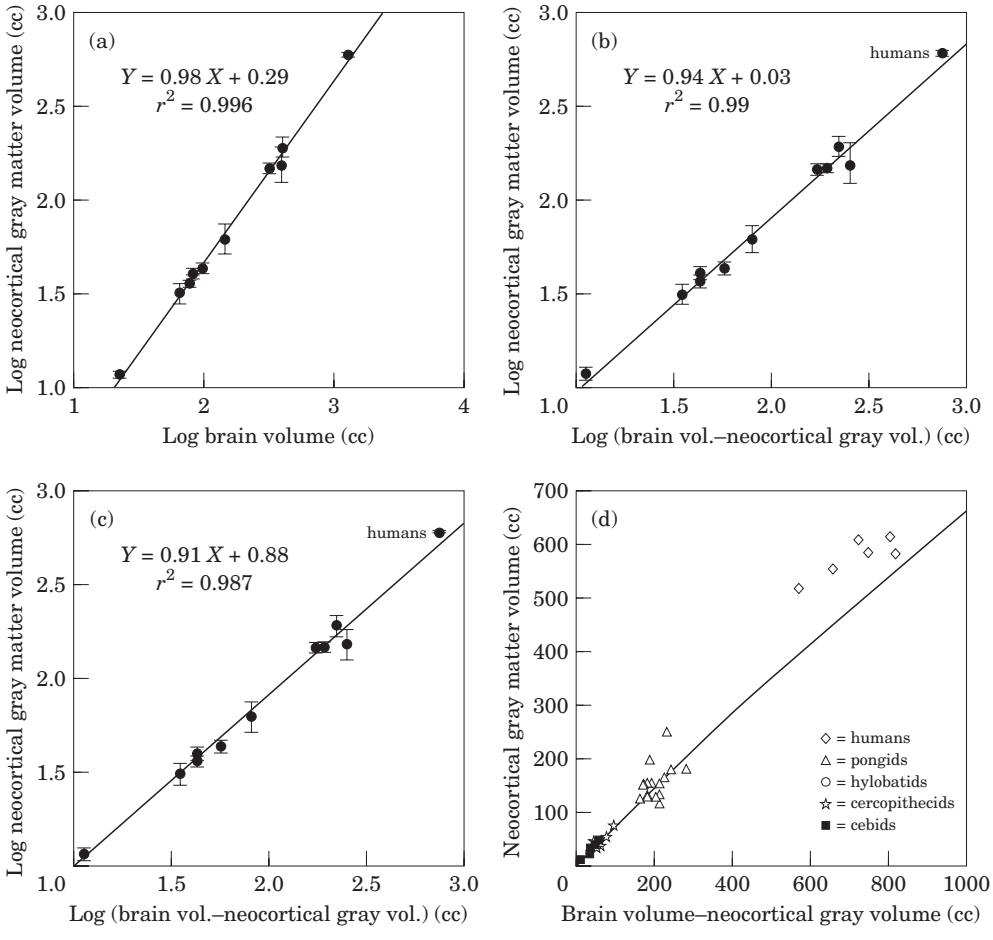

Figure 4. Allometric relationship between neocortical gray matter and brain volume. (a) Logarithmic plot of neocortical gray matter volume *vs.* brain volume with regression line fit through all 11 species of anthropoid primates; (b) logarithmic plot of neocortical gray matter volume *vs.* the volume of the rest of the brain with regression line fit through all 11 species of anthropoid primates; (c) logarithmic plot of neocortical gray matter volume *vs.* the volume of the rest of the brain with regression line fit through ten nonhuman primate species; (d) plot of neocortical gray matter volume *vs.* the volume of the rest of the brain for 44 anthropoid primate subjects with curve fit through the 38 nonhuman primate subjects.

accurately when the data are plotted in non-logarithmic coordinates. In Figure 4(d), data from individual subjects (rather than species' means) are plotted and a curve is fit through the nonhuman primate sample. All six human data points lie well above the curve, demonstrating that the human neocortex is larger than expected for a primate of our brain size (minus neocortical gray matter).

Cerebral white matter volume

In Figure 5(a), log cerebral white matter volume is plotted *vs.* log brain volume. The slope of the least-squares regression line through the 11 species data points is significantly greater than 1 (95% C.I.=1·04, 1·14), indicating that the relationship is positively allometric. Increases in cerebral white matter volume outpace increases in total brain volume. However, cerebral white

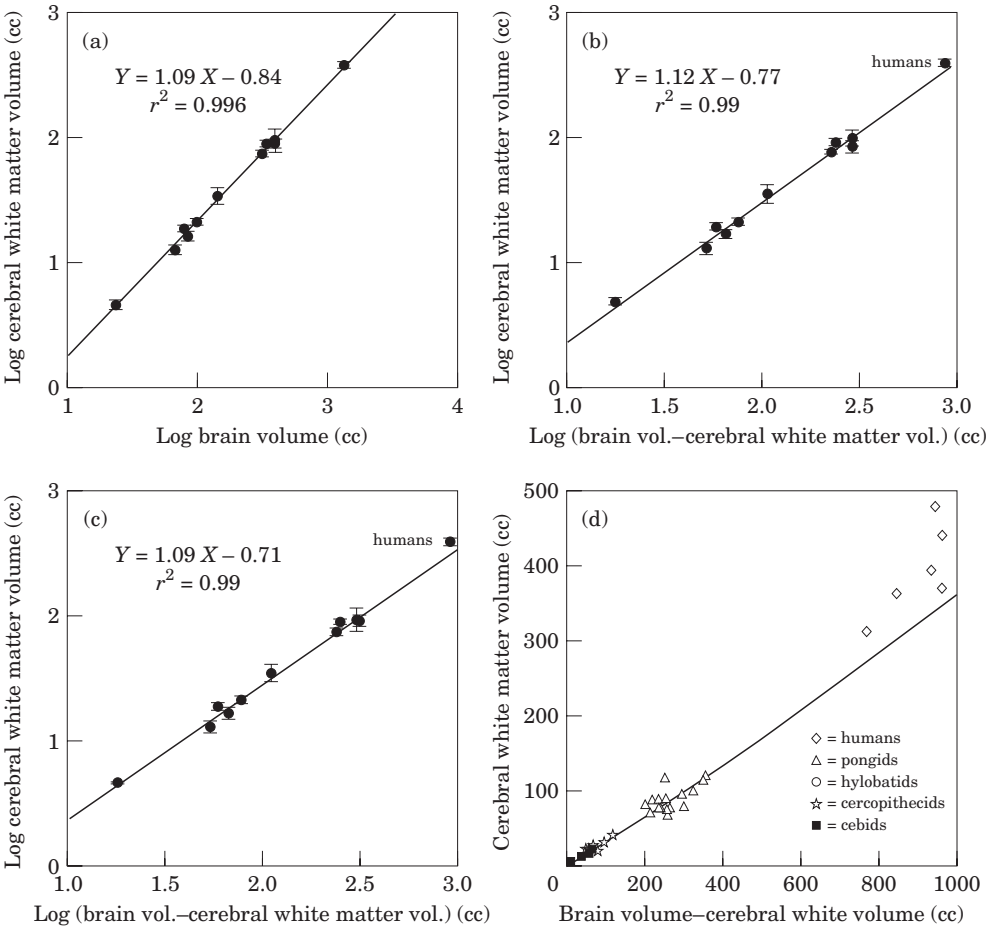

Figure 5. Allometric relationship between cerebral white matter and brain volume. (a) Logarithmic plot of cerebral white matter volume *vs.* brain volume with regression line fit through all 11 species of anthropoid primates; (b) logarithmic plot of cerebral white matter volume *vs.* the volume of the rest of the brain with regression line fit through all 11 species of anthropoid primates; (c) logarithmic plot of cerebral white matter volume *vs.* the volume of the rest of the brain with regression line fit through ten nonhuman primate species; (d) plot of cerebral white matter volume *vs.* the volume of the rest of the brain for 44 anthropoid primate subjects with curve fit through the 38 nonhuman primate subjects.

matter constitutes between 20 and 31% of total brain volume in our sample so that Figure 5(a) also involves the regression of a substantial part of a variable on itself. To alleviate this problem, cerebral white matter is plotted *vs.* the volume of the rest of the brain (total brain volume–cerebral white matter volume) in Figure 5(b). The slope increases from 1·09 in Figure 5(a) to 1·12 (95% C.I.=1·05, 1·19). For none of the 11 species is the observed cerebral white matter volume significantly different from that predicted by the regression line. When humans are excluded from the regression [Figure 5(c)], the slope decreases to 1·09 (95% C.I.=1·00, 1·18), suggesting that the strong leverage of the human data point has a substantial impact on the slope of the regression line. In this analysis, humans are the only species with an observed cerebral white

matter volume significantly different from the expected volume. Specifically, it is 22% (or 60 cc) larger than expected. The discrepancy between the observed and expected human cerebral white matter volume can be perceived more accurately when the data are plotted on non-logarithmic coordinates. In Figure 5(d), data from individual subjects are plotted and a curve is fit through the nonhuman primate sample. All six human data points lie above the curve, demonstrating that the human cerebral white matter volume is larger than expected for a primate of our brain size (less cerebral white matter).

Neocortical gray plus cerebral white matter volume

In the most widely cited database on comparative primate neuroanatomy (Stephan *et al.*, 1981), neocortical volume measurements include both neocortical gray matter and cerebral white matter. To make our analyses comparable to those conducted previously with this data set, we repeat the above analyses using the combined volume of neocortical gray matter plus cerebral white matter. In Figure 6(a), this sum (labeled ''neocortex'') is regressed on total brain volume and a regression line is fit through the 11 species' data points. The slope (1·00) suggests an isometric relationship, however the variable on the *y*-axis constitutes between 61 and 75% of that on the *x*-axis. Therefore, in Figure 6(b), neocortical volume (gray plus white) is regressed on the volume of the rest of the brain. The slope (0·99) indicates that the neocortex increases at about the same pace as the rest of the brain. Analysis of residuals off the regression line in Figure 6(b) reveals that both humans and squirrel monkeys have significantly more ''neocortex'' than predicted by the regression line, whereas mangabeys have significantly less. The human neocortex (gray plus white matter) is 35% (or 254 cc) larger than expected for a primate of the same brain size (minus the neocortex). When humans are excluded from the regression, the slope decreases to 0·92 [Figure 6(c)], and humans become the only species with significantly more neocortex than predicted by the regression line. Mangabeys are the only species with significantly less. In this analysis, the human neocortex is 61% (or 370 cc) larger than expected for an anthropoid primate of the same brain size (less neocortex). As with the other analyses, the discrepancy between the observed and expected human neocortical volume can be perceived more accurately when the data are plotted on nonlogarithmic coordinates. In Figure 6(d), data from individual subjects are plotted and a curve is fit through the nonhuman primate sample. All six human data points lie above the curve, demonstrating that the human neocortex is larger than expected for a primate of our brain size (minus neocortex).

Neocortical gray vs. *cerebral white matter*

To test the hypothesis that increases in cerebral white matter volume outpace increases in neocortical gray matter volume among anthropoid primates, cerebral white matter is regressed against neocortical gray matter in Figure 7. The slope of the regression line is 1·12 (95% C.I.=1·05, 1·19), providing support for the hypothesis.

Gyrification

Gyrification indices indicate how much of the neocortex is buried within cerebral sulci. They provide a measure of the amount of cortical folding (see Methods). Mean whole brain gyrification indices for each species are provided in Table 6. To determine if gyrification is related to brain size in our sample, whole brain gyrification indices are plotted *vs.* log brain volume in Figure 8. There is a statistically significant positive correlation between brain volume and GI (r-square=0·92; $P<0·001$), indicating that larger brains are more convoluted.

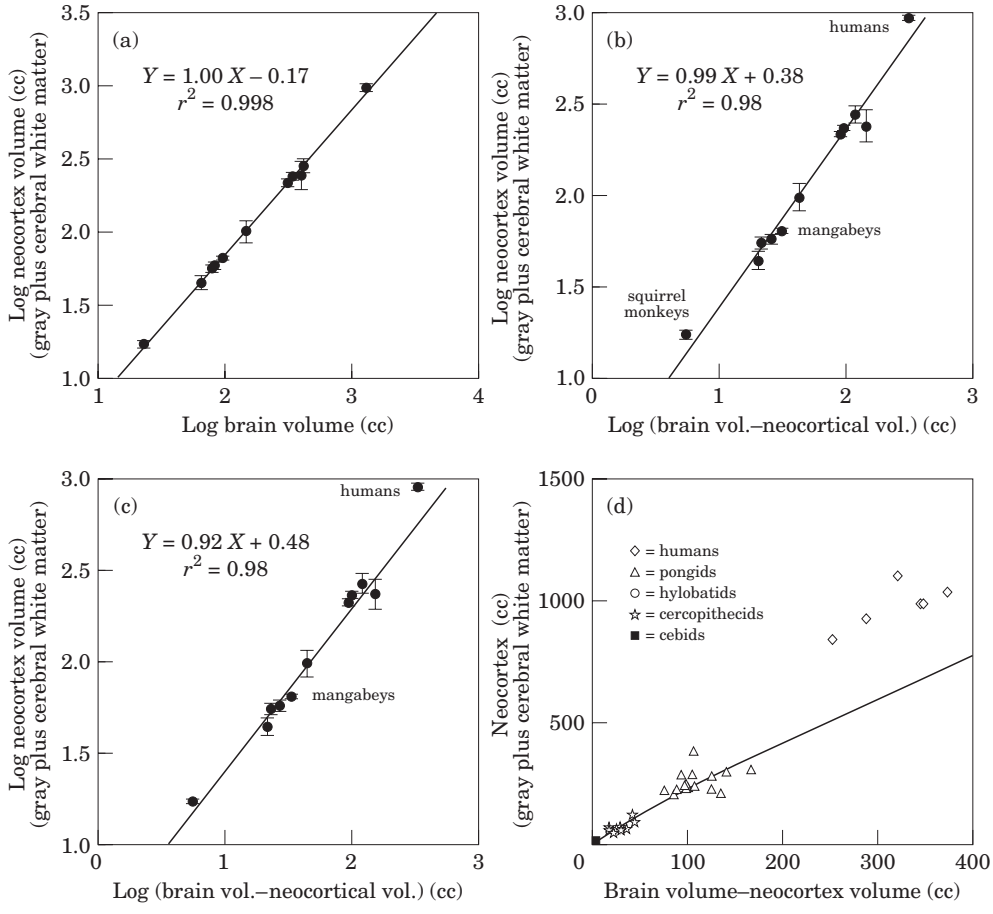

Figure 6. Allometric relationship between neocortex (gray plus cerebral white matter) and brain volume. (a) Logarithmic plot of neocortical volume *vs.* brain volume with regression line fit through all 11 species of anthropoid primates; (b) logarithmic plot of neocortical volume *vs.* the volume of the rest of the brain with regression line fit through all 11 species of anthropoid primates; (c) logarithmic plot of neocortical volume *vs.* the volume of the rest of the brain with regression line fit through ten nonhuman primate species; (d) plot of neocortical volume *vs.* the volume of the rest of the brain for 44 anthropoid primate subjects with curve fit through the 38 nonhuman primate subjects.

Capuchin monkeys are the only species in which the observed gyrification index is significantly different from that predicted by the regression line. Capuchin brains are less gyrified than expected for a typical anthropoid brain of the same size.

To determine whether the regional pattern of gyrification across the brain varies by species, gyrification indices were calculated for each of ten equally spaced coronal slices in each brain. Species were grouped by families and the mean index for each slice of each family is plotted in Figure 9. Slices are arranged along the rostral–caudal dimension of the brain such that the first slice is 1/11 the distance from the rostral to the caudal pole of the brain, the second is 2/11 that distance, and so on. As expected from Figure 8, the largest brained families (e.g., hominids) have the highest indices across all slices. The overall pattern of gyrification is quite similar in all families. In general,

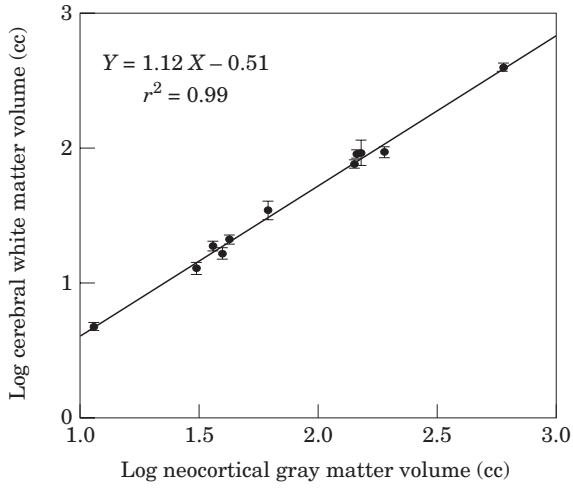

Figure 7. Allometric relationship between cerebral white matter and neocortical gray matter. Logarithmic plot of cerebral white matter *vs.* neocortical gray matter with regression line through 11 species of anthropoid primates.

Table 6 Whole brain gyrification indices (GI) in 11 species of anthropoid primates

Species (mean ± S.E.)	Whole brain gyrification index
H. sapiens	2·57 ± 0·04
P. paniscus	2·17 ± 0·03
P. troglodytes	2·19 ± 0·01
G. gorilla	2·07 ± 0·03
P. pygmaeus	2·29 ± 0·08
H. lar	1·90 ± 0·03
P. cynocephalus	2·03 ± 0·06
M. mulatta	1·73 ± 0·02
C. atys	1·84 ± 0·05
C. apella	1·60 ± 0·03
S. sciureus	1·56 ± 0·04

cortical folding increases caudally, peaks in the ninth coronal slice, and then declines in the tenth. The ninth slice typically cuts through the parieto-occipital sulcus on the medial surface of the brain, and the tenth is always in the occipital lobe.

As with the whole brain GI, the GI of each coronal slice was regressed on brain volume to determine if the two are related and if any of the 11 species depart from the allometric regression line. GIs for all ten slices are positively associated with brain volume. The slope and *r*-square value for each of the regressions is provided in Table 7. The ninth coronal slice has the largest slope, suggesting that this region of the cortex becomes most gyrified with increasing brain size. On the other hand, the seventh coronal slice has the shallowest slope, suggesting that this region of the cortex experiences the smallest increase in gyrification as brain size increases. The seventh coronal slice typically cuts through the splenium and near the posterior limit of the central sulcus where it approaches midline to the brain. Table 8 provides the slice number and species for slices that are significantly more or less gyrified than predicted by the regression line for that slice. Of the 110 slices (11 species × 10 slices), 15 were significantly different from the prediction of the regression line (six would be expected by chance alone). Squirrel monkey brains appear to be uniquely gyrified in the first coronal slice (through the prefrontal lobe). However, this result should be interpreted with caution. The nonhuman primate regression line predicts a gyrification index of 0·91 for squirrel monkeys in

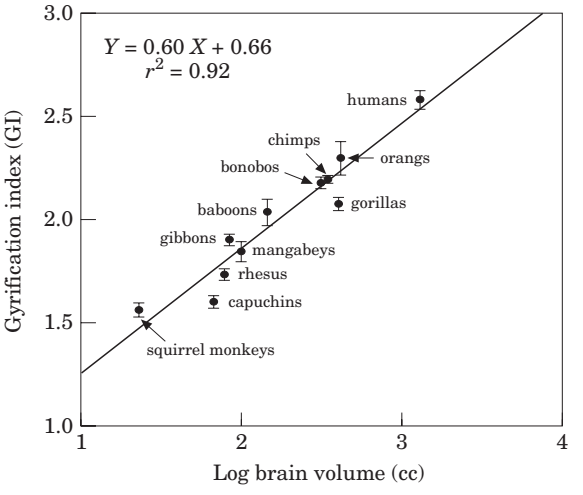

Figure 8. Allometric relationship between whole brain gyrification indices (GI) and brain volume. Plot of whole brain gyrification indices *vs.* log brain volume with regression line fit through 11 species of anthropoid primates.

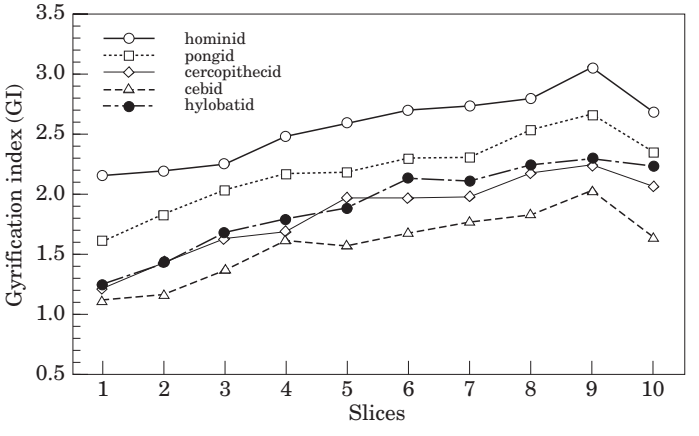

Figure 9. Pattern of gyrification across the anterior–posterior dimension of the brain in five families of anthropoid primates. Each data point represents the mean gyrification index for all subjects of a specific family for a specific slice. Coronal slice no. 1 is 1/11 the distance from the anterior to the posterior pole of the brain, coronal slice no. 2 is 2/11 that distance, and so on. The tenth coronal slice is the most caudal slice and cuts through the occipital lobe in all five families.

the first coronal slice, based on their brain volume. However, a gyrification index cannot be less than 1. This suggests that the function relating GI and brain volume may not be log-linear when brain volume decreases below a certain threshold. All primate brains must have GIs greater than 1 since all possess both a sylvian and a calcarine fissure (Smith, 1902; Martin, 1973). Therefore, the slope of the regression is probably altered for smaller anthropoid brains. Squirrel monkey brains are also more gyrified than expected in the fourth coronal slice which cuts through the posterior frontal lobe and the amygdala in the anterior temporal lobe.

Table 7 Slopes and *r*-square values relating gyrification indices and brain volume in ten coronal slices

Slice	Logarithmic slope	r^2
1	0·61	0·88
2	0·64	0·92
3	0·58	0·89
4	0·57	0·74
5	0·56	0·77
6	0·61	0·88
7	0·53	0·81
8	0·61	0·86
9	0·66	0·93
10	0·63	0·7

Since whole brain GI for capuchins is significantly lower than expected for their brain size, it is expected that some or all of the ten coronal slices in the capuchin brain will be less gyrified than predicted by the regression line. Table 8 shows that the deficit in gyrification in the capuchin brain is concentrated in the anterior half of the brain (i.e., slices 1, 2, 3 and 5). Mangabeys are less gyrified than expected in the first (prefrontal) and second coronal slices. The second slice is in the anterior frontal lobe and cuts through the anterior cingulate gyrus. Baboons are more gyrified than expected in the third (frontal lobe; genu of the corpus callosum) and eighth (parietal and posterior temporal lobe) coronal slices. Chimpanzees are more gyrified than expected in the third coronal slice (through the genu in the frontal lobe and the anterior tip of the temporal lobe). Rhesus macaques are significantly less gyrified than predicted in the fourth coronal slice (through the frontal lobe and the amygdala in the temporal lobe). Gorillas are less gyrified than predicted in the ninth coronal slice (posterior parietal and anterior occipital lobe). Finally, both gibbons and orang-utans are significantly more gyrified than expected in the tenth coronal slice (through the occipital lobe).

None of the slices through the human brain departed from the allometric regression line for its respective slice. However, the human data point has substantial leverage in all of these analyses so that it may be more appropriate to fit the regression line through the 10 nonhuman species. When this is done, humans have a larger GI than expected in slices 1 and 7 (Figure 10). Slice 1 cuts through the prefrontal lobe in all species. Thus, our results support the hypothesis that the human prefrontal cortex is more gyrified than expected for a primate of our brain size. Figure 11 illustrates the first coronal slice from one representative of each of the 11 species in our sample, and Figure 12 shows the seventh coronal slice. In none of the ten slices is the human brain significantly less gyrified than predicted by the nonhuman primate regression line.

Discussion

Relative brain size

Slope. The logarithmic slope relating brain volume and body weight in our sample is 0·64 (95% C.I.=0·54, 0·74) using actual body weights and 0·59 (95% C.I.=0·49, 0·69) using published body weights. Using post-mortem brain specimens, Stephan and colleagues (Stephan *et al.*, 1988) reported a slope of 0·70 for 48 species of nonhuman simians. This value falls within the 95% confidence interval for our slope with actual body weights but just outside the interval for our slope with published body weights. The absence of callitrichid primates from our sample could explain the discrepancy between our MRI and the post-mortem slope. Among anthropoids, callitrichids have small brains for their body size (Jerison, 1973; Stephan *et al.*, 1988). Because they are also small-bodied primates, the callitrichid data points would tend to pull the left end of the regression line down, thereby increasing its slope. Adding callitrichid primates to our sample might therefore be expected to increase our slope, making it closer to 0·70.

Table 8 Coronal slices that are more or less gyrified than expected from brain volume

Species	Slice	> or < Expected	Expected	Observed with 95% C.I.
Squirrel	1	>	0·91	1·13 (1·12, 1·14)
Squirrel	4	>	1·43	1·56 (1·44, 1·68)
Capuchin	1	<	1·19	1·11 (1·05, 1·17)
Capuchin	2	<	1·34	1·18 (1·12, 1·24)
Capuchin	3	<	1·55	1·39 (1·27, 1·51)
Capuchin	5	<	1·81	1·54 (1·49, 1·59)
Mangabey	1	<	1·3	1·22 (1·16, 1·28)
Mangabey	2	<	1·83	1·76 (1·57, 1·95)
Baboon	3	>	1·74	1·78 (1·78, 1·78)
Baboon	8	>	2·28	2·46 (2·40, 2·52)
Chimpanzee	3	>	1·96	2·07 (2·00, 2·14)
Rhesus	4	<	1·73	1·51 (1·34, 1·68)
Gorilla	9	<	2·71	2·57 (2·44, 2·70)
Orang-utan	10	>	2·42	2·78 (2·57, 2·99)
Gibbon	10	>	1·99	2·23 (2·15, 2·31)

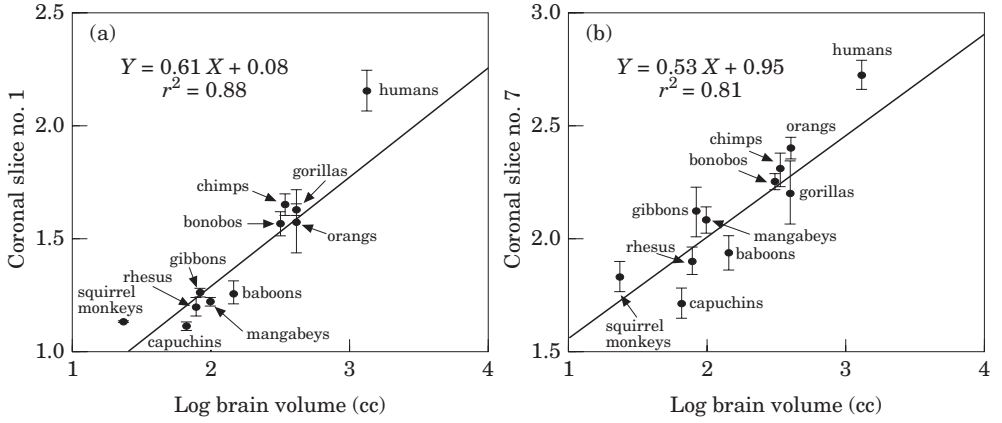

Figure 10. Regions of increased gyrification in the human brain. (a) Plot of the gyrification index for the first coronal slice *vs.* log brain volume with regression line fit through ten species of nonhuman primates; (b) plot of gyrification index for the seventh coronal slice *vs.* log brain volume with regression line fit through ten species of nonhuman primates.

Species differences. Using actual body weights, our data show that the human brain is 3·4 times larger than expected for an anthropoid primate of the same body size. Using published body weights, it is 4·3 times larger. Analysis of the post-mortem data of Stephan and colleagues (1970) indicates that the human brain is 3·1 times larger than expected for an anthropoid primate of the same body size (Falk, 1980). Our data generate a larger value because our observed human brain volume (1298·8 cc, $n=6$) is larger than that of the human brain in the post-mortem data set (1251·85 cc, $n=1$) and our expected human brain volume (372·9 cc) is smaller than theirs (403·7 cc). The latter difference is a consequence of the shallower slope for our regression line which, as just mentioned, is probably due to the lack of callitrichid subjects in our sample. Our data also demonstrate that the human brain is significantly larger than

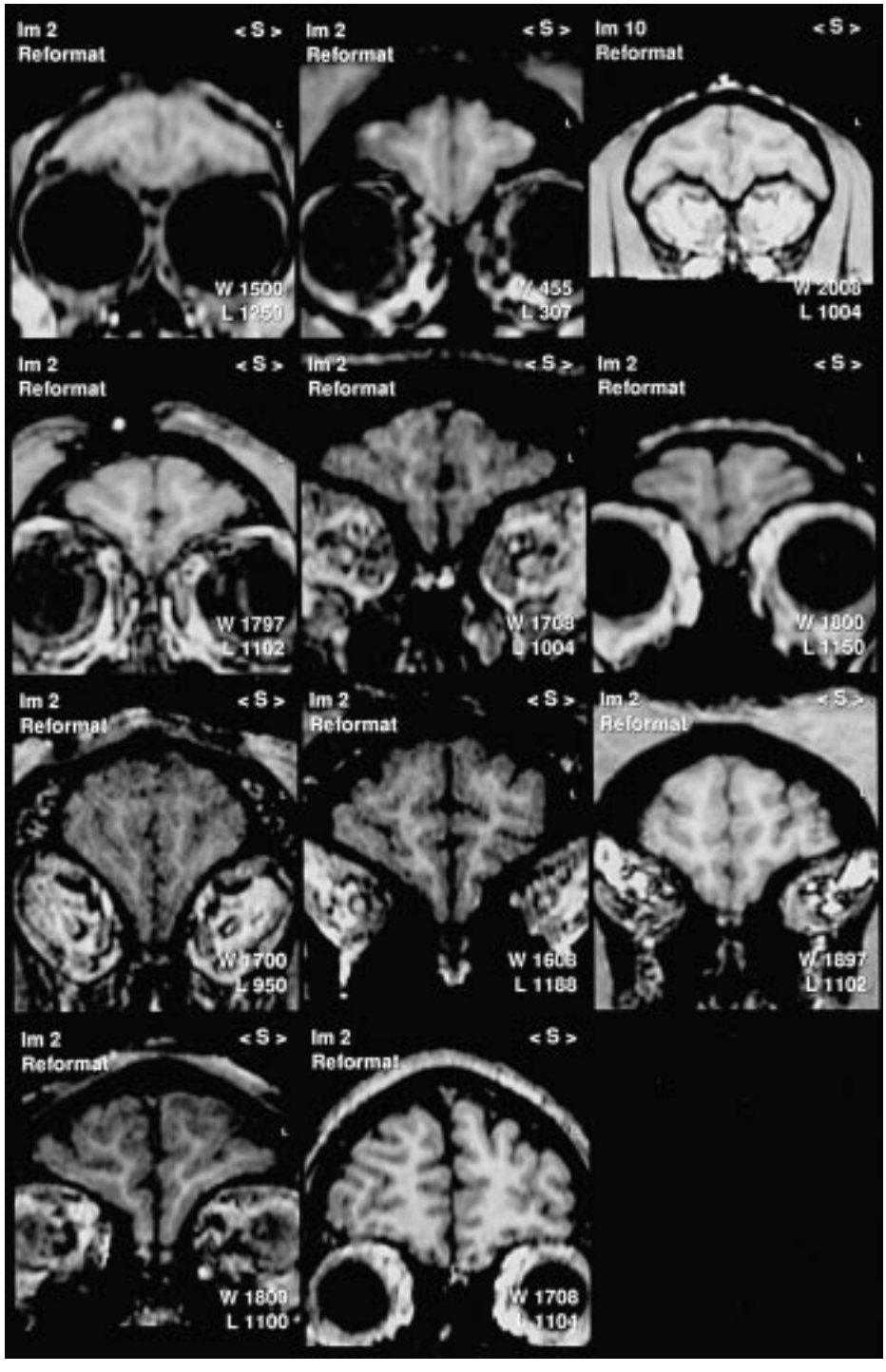

Figure 11. The prefrontal lobe in 11 species of anthropoid primates. First coronal slice in one representative from each of 11 species of anthropoids. Species are presented in the following order (from top left moving across the row): squirrel monkey (*S. sciureus*), capuchin monkey (*C. apella*), rhesus macaque (*M. mulatta*), sootey mangabey (*C. atys*), baboon (*P. cynocephalus*), gibbon (*H. lar*), orang-utan (*P. pygmaeus*), gorilla (*G. gorilla*), chimpanzee (*P. troglodytes*), bonobo (*P. paniscus*), human (*H. sapiens*).

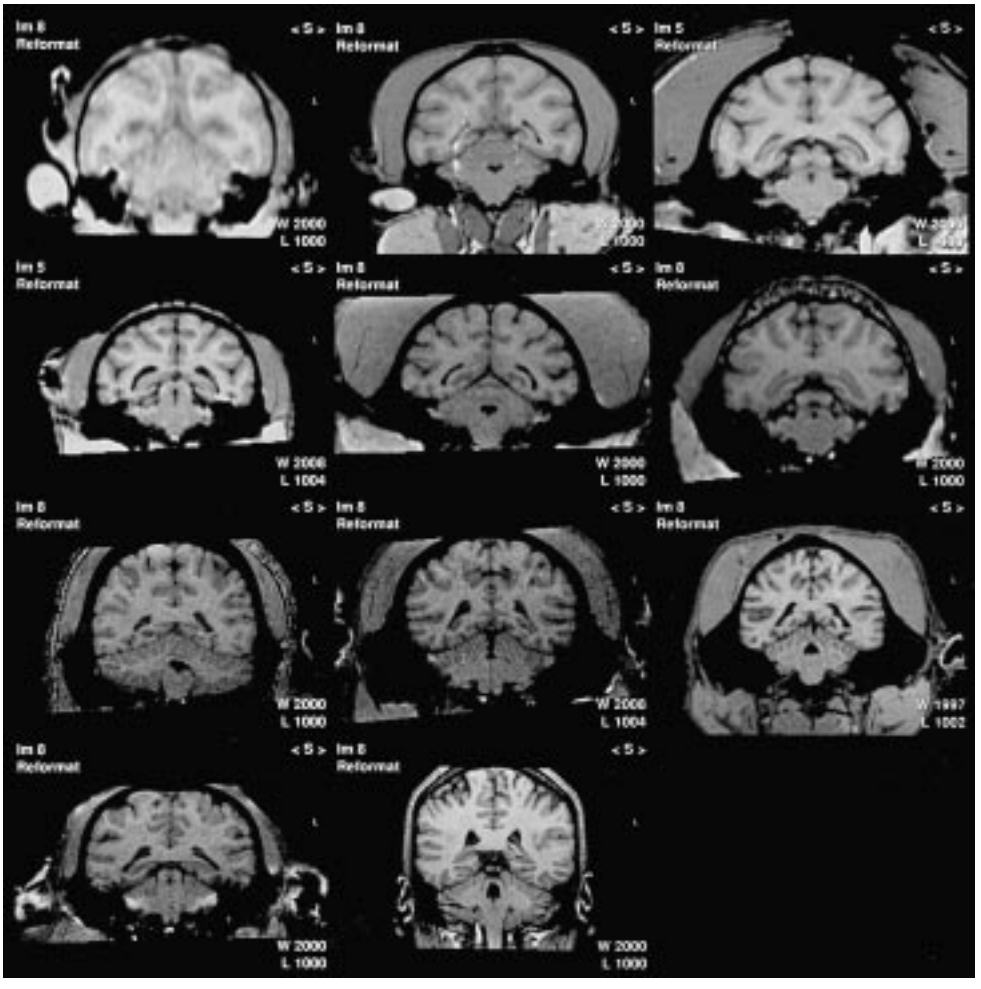

Figure 12. The parietal/posterior temporal lobe in 11 species of anthropoid primates. Seventh coronal slice in one representative from each of 11 species of anthropoids. Species are presented in the following order (from top left moving across the row): squirrel monkey (*S. sciureus*), capuchin monkey (*C. apella*), rhesus macaque (*M. mulatta*), sootey mangabey (*C. atys*), baboon (*P. cynocephalus*), gibbon (*H. lar*), orang-utan (*P. pygmaeus*), gorilla (*G. gorilla*), chimpanzee (*P. troglodytes*), banobo (*P. paniscus*), human (*H. sapiens*).

expected for a primate of the same spinal cord area. This might reflect a greater surplus of neural tissue beyond that required to process basic sensorimotor information (Passingham, 1982).

Using Jerison's encephalization quotient (EQ) values derived from post-mortem brain specimens (Jerison, 1973), there is no obvious difference in relative brain size between monkeys and apes (mean ape EQ=2·12, n=7; mean monkey EQ=2·08, n=39). However, using Stephan's encephalization indices (EIs), apes do appear more encephalized than monkeys (mean ape EI=10·2, n=3; mean monkey EI=7·7, n=23). Other researchers, using various measures of relative brain size, have also reported apes to be more encephalized than monkeys (Hemmer, 1966; Clutton-Brock & Harvey, 1980; Passingham, 1982).

In Tables 2 and 3, ER and ED values for great apes are generally higher than for monkeys. The exceptions are capuchin monkeys and gorillas (but only when published body weights are used for gorillas). Thus, our results suggest that great apes typically have larger brains for their body size than monkeys.

Capuchin monkeys have been previously demonstrated to be highly encephalized compared with other monkeys (Jerison, 1973; Stephan *et al.*, 1988). Although in our analysis the capuchin brain is not significantly larger than expected for a primate of the same body size, this is merely a consequence of a limitation in the statistical power of our analysis. The ER and ED scores from Tables 2 and 3 show that capuchins are clearly more encephalized than other monkeys. Based on ER scores, capuchins are on a par with the great apes in terms of relative brain size. However, based on ED scores, capuchins appear less encephalized than the great apes (excepting gorilla). These results imply that although capuchins do not have as much ''extra'' brain tissue as the great apes, they have a similar amount of extra tissue as a percentage of their expected brain volume. In contrast to the analyses with body weight as the independent variable, capuchins do not appear uniquely encephalized when brain size is regressed on spinal cord area. These results are interesting in view of capuchins' highly developed skills in object manipulation (Parker & Gibson, 1977; Beck, 1980; Visalberghi, 1990; Fragaszy & Adams-Curtis, 1991; Westergaard, 1994). A regression of spinal cord area on body weight reveals that capuchins have large spinal cords for their body size. Thus, it is possible that the object manipulation skills of capuchin monkeys are supported by an augmented number of sensorimotor fibers coursing through the spinal cord, as well as an enlarged brain.

Using actual body weights, rhesus monkeys have smaller brains than expected for their body size. However, when published body weights are used, they do not appear underencephalized. These results suggest that our rhesus monkey subjects are overweight; they have large bodies for their brain size rather than small brains for their body size. Nevertheless, rhesus have significantly smaller brains than expected for their spinal cord area which suggests that they are underencephalized compared with the rest of our sample.

Although bonobo brains are not significantly larger than expected for their body size, they are significantly larger than expected for their spinal cord area. Bonobos also have significantly smaller spinal cords than expected for their body size. Thus, they appear overencephalized, not because of their large brain size, but because of their small spinal cord area.

Although the difference is not statistically significant due to the small sample size, gorillas appear underencephalized using published body weights but not with actual body weights. Our actual body weight for gorillas is derived from one adult female and one subadult male (aged 8 years). The male had probably completed brain growth but not body growth at the time he was scanned. Thus, the published body weight estimate is probably more representative of the true adult male gorilla mean that is our actual body weight. It has been suggested that gorillas appear to have a small relative brain size because they are scaling along the pongid allometric curve which is shallower than that of the reference line used to calculate relative brain size. In other words, gorillas are ''allometrically enlarged chimpanzees'' (Pilbeam & Gould, 1974). If this is true, then gorillas have the brain:body proportions expected for a pongid of their size. To test this hypothesis, our pongid data are plotted in Figure 13. The solid regression line is fit through the bonobo, chimpanzee, and orang-utan data points. For these three species, actual body weights are used

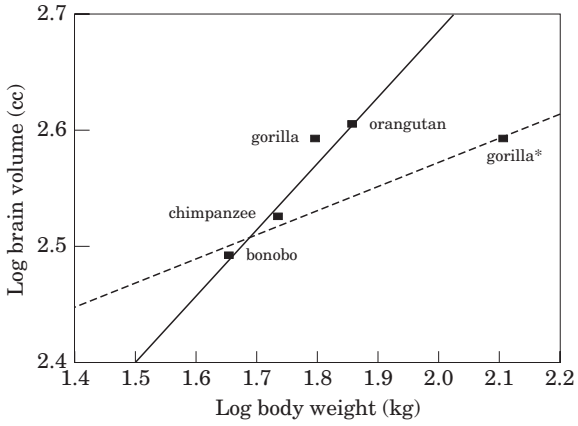

Figure 13. Relative brain size among pongids. Logarithmic plot of brain volume *vs.* body weight for pongids. All species data points are based on actual body weights with the exception of "gorilla*" which is based on the published mean body weight for gorillas. The solid line is the least-squares regression line through the bonobo, chimpanzee, and orang-utan data points. The dashed line is the least-squares regression line through the bonobo, chimpanzee and gorilla* data points.

(rather than published species' means). When actual body weights are used for gorillas, they do not obviously depart from this regression line (data point labeled "gorilla" in Figure 13). In other words, they appear to be scaling along the pongid allometric curve. However, for the reason just mentioned, the actual body weight for our gorilla sample underestimates the true adult gorilla body weight. Therefore, a second data point is plotted for our gorilla sample (labeled "gorilla*") based on the published body weight estimate from Harvey *et al.* (1987). This point clearly departs from the regression line fit through the other three pongid species (the solid line). However, this graph could also be interpreted as reflecting a departure from allometry in orang-utans if the regression line is fit through the African great apes (dotted line in Figure 13). In this case, orang-utans would stand out among the pongids by virtue of their large relative brain size. We believe that the most likely explanation for these data is that gorillas have unusually large bodies for their brain size resulting from excessive body growth that occurs late in development. In this case, it would be inappropriate to consider them allometrically enlarged chimpanzees.

Neocortical gray and cerebral white matter

Relative neocortical volume. The results for relative neocortical volume largely parallel those for relative brain size: the logarithmic slope for the regression on body weight is equal to 0·61, humans have significantly larger neocortices than expected for a primate of their body size, rhesus macaques have significantly smaller neocortices than expected for their body size, and apes generally have larger relative neocortex sizes (as measured by NR and ND from Table 5) than monkeys, with the exception of capuchin monkeys and gorillas who have larger and smaller neocortices than expected for their phylogenetic status, respectively. The similarity in relative brain size and relative neocortex size comparisons suggests that brain volume and neocortical volume may be directly proportional to each other. Since our slope for the logarithmic regression of neocortical gray matter on brain volume is not significantly different from 1·00 (see Figure 3), this possibility cannot be rejected.

Scaling of neocortical gray and white matter. Our results show that cerebral white matter scales at a higher power of brain volume than does neocortical gray matter (compare slopes in Figures 4 and 5, and Figure 7), and support the hypothesis that increases in cerebral white matter outpace increases in neocortical gray matter. The same observation has been made with post-mortem material (Frahm *et al.*, 1982), where the slope for the logarithmic regression of cerebral white matter on neocortical gray matter is 1·28 (1·20, 1·36) for a sample of 13 nonhuman anthropoids. This slope is steeper than that reported here for living specimens (1·12; 95% C.I.=1·05, 1·19) and suggests a larger increase in white matter relative to gray matter as brain size increases. Differential shrinkage of gray and white matter in the post-mortem specimens (Kretschmann *et al.*, 1982) could contribute to the difference in slopes.

Since white matter is composed of axons and gray matter is largely composed of neuronal cell bodies, these data might be relevant to the scaling relationship between neocortical neuron number and the number of connecting axons. If neocortical neuron number is related to neocortical volume in the same way that axon number is related to cerebral white matter volume, then our data indicate that increases in the number of connections between neocortical neurons outpaces increases in the number of neocortical neurons. Nevertheless, the increase in white matter is probably not sufficient to maintain the same amount of connectivity among neocortical neurons as the number of neurons increases. Frahm and colleagues (1982) estimated that the number of white matter connections would need to grow at the square of the number of neurons in order to preserve connectivity in a maximally connected network in which each neuron was connected to every other one. Our slope is significantly less than 2. Although the neocortex is not a maximally connected network, these data suggest that the proportion of all neocortical neurons that a given neuron is connected with probably decreases as the number of neurons increases. Deacon (1990) has speculated that it is long-distance connections that are preferentially culled with increasing brain size, and that this forces larger brains to process more information in local networks.

Neocortex size in relation to brain size. The allometric curves in Figures 3(d), 4(d), and 5(d) describe how the anthropoid brain grows; they describe rules of brain growth. Departures from these curves suggest that natural selection may have acted to displace species from the allometric curve. The fact that humans depart significantly from the allometric curves in Figures 3(d), 4(d), and 5(d) suggest that brain expansion throughout hominid evolution did not follow a predictable allometric trend. In other words, selection for a global increase in brain size that acted uniformly on every brain structure appears not to have occurred. Instead, these graphs suggest that there was direct, specific selection for expansion of both neocortical gray matter and cerebral white matter in the hominid lineage. Thus, our results support the hypothesis that the human neocortex is larger than expected for a primate of our brain size.

The post-mortem data set of Stephan and colleagues (1988) can also be analyzed to determine if the human neocortex is larger than predicted by nonhuman primate allometric trends. A regression line was fit through a logarithmic plot of neocortical volume *vs.* the volume of the rest of the brain for the 26 nonhuman simian species in the data set. Consistent with our MRI results, the observed human neocortical volume is 18% or 155 cc larger than predicted by the regression line. The statistical significance of this departure from allometric predictions cannot be evaluated because the human

Table 9 Comparison of gyrification indices (GI) obtained with MRI and with post-mortem brain specimens

Species	MRI GI	Post-mortem GI*
H. sapiens	2·57	2·56
P. paniscus	2·17	na
P. troglodytes	2·19	2·43
G. gorilla	2·07	2·26
P. pygmaeus	2·29	2·32
H. lar	1·9	1·86
P. cynocephalus	2·03	2·07
M. mulatta	1·73	1·81
C. atys	1·84	na
C. apella	1·6	1·69
S. sciureus	1·56	1·49

na=not available.
*=data from Zilles *et al.*, 1989.

data point is based on only a single brain specimen.

Gyrification

MRI scans lack cytoarchitectonic information and, in most cases, cytoarchitectonic areas cannot be consistently and reliably inferred from the external surface anatomy of the brain. Consequently, comparing the size of functional cortical areas across species is problematic. The gyrification index used in this study compares cortical regions based on their rostral–caudal position, independent of their position with respect to surface anatomy features (i.e., sulci and gyri). The gyrification index makes no assumptions about the functional homology of slices being compared across species.

Our whole brain gyrification indices are in good agreement with those derived from post-mortem brain specimens (Zilles *et al.*, 1989). Table 9 lists the values obtained in each study for the nine species that were represented in both (*Cebus albifrons* was substituted for *Cebus apella* for the post-mortem data). The two sets of values correlate at $r=0{\cdot}96$ ($P<0{\cdot}001$). In our study, we confirm the observation that larger anthropoid primate brains are more convoluted than smaller ones (Bonin, 1941*b*; Elias & Schwartz, 1971; Jerison, 1982; Zilles *et al.*, 1989). The slope we report here (0·60) agrees well with that reported for anthropoids using post-mortem specimens (0·66; Zilles *et al.*, 1989). Why should larger primate brains be more convoluted? As brain size increases among primates, cortical thickness increases minimally whereas cortical surface area increases substantially. This suggests that the cortex grows like an expanding sheet that covers the brain. One proposal to account for cortical folding is that, as this cortical sheet expands, it must fold in order to fit within the confines of a spherically shaped skull (Jerison, 1982; Hofman, 1989; Essen, 1997). Alternatively, it has been suggested that factors intrinsic to the cortex may cause it to fold. For example, Richman and colleagues (1975) proposed that greater expansion of outer *vs.* inner cortical layers was responsible for folding. However, this model does not readily explain why larger brains should necessarily be more convoluted. Van Essen (1997) suggested that tension along axons produces gyri between strongly connected cortical regions and sulci between weakly connected regions. As the cortex expands, folds might allow interconnected cortical regions to remain in close spatial proximity with one another so that the length and diameter of white matter connections can be minimized. This might be at an evolutionary premium because of the high metabolic costs of neural tissue and, in humans, the constraints the birth canal imposes on brain size.

Our data indicate that the brain of the capuchin monkey (*Cebus apella*) is significantly less gyrified than expected for a typical anthropoid brain of the same size. From Zilles *et al.*'s (1989) plot of GI *vs.* log brain weight, it is apparent that capuchins (*Cebus albifrons*) also lie below the regression line in their analysis. What is the significance of a species possessing a more or less gyrified brain than expected for its brain size? If

gyrification is a function of the size of the neocortical surface in relation to the size of the skull, then capuchins should have a large skull in relation to their neocortical surface area. On the other hand, if gyrification results from differential expansion of the outer and inner cortical layers (as proposed by Richman *et al.*, 1975), then capuchins should have a smaller discrepancy in the growth of the outer and inner cortical layers. Since the outer cortical layers typically send axonal projections to other cortical areas, whereas the inner cortical layers send most of their projections away from the cortex (Zilles *et al.*, 1989), the low GI of the capuchin brain could represent reduced growth of the outer cortical layers and reduced intracortical connectivity. Alternatively, it might represent increased growth of the inner cortical layers and an augmentation of descending projections.

A pattern of gyrification similar to that observed in Figure 9 has been reported for anthropoid primates using post-mortem brains (Zilles *et al.*, 1988): a continuous increase in GI over the frontal and temporal lobes that reaches a maximum over the posterior parietal and anterior occipital lobe and then declines in the occipital lobe. The post-mortem data suggest that the discrepancy between human and nonhuman values is greatest in the anterior (specifically the prefrontal) part of the brain, and minimal in the caudal regions of the brain. Our own data from living primates suggest that the difference between humans and nonhuman anthropoids is quite uniform across the brain with the exception of the first and seventh coronal slices for which the discrepancy is greater (discussed more below).

The slices listed in Table 8 are all significantly more or less gyrified than expected for their brain size. As with whole brain gyrification indices, when individual slices are more gyrified than expected for their brain size, it may reflect increased intracortical processing in those areas of the brain. However, one must be cautious in drawing functional interpretations from these data. First, as mentioned above, six of the slices listed in Table 8 are expected to be type 1 errors. Second, it is difficult—and often impossible—to assign functions to the brain regions corresponding to the ten coronal slices.

Because the first coronal slice cuts through the prefrontal cortex in all species, our results show that the human prefrontal cortex is significantly more gyrified than expected for a nonhuman anthropoid primate of the same brain size (see Figure 10). Zilles and colleagues (1988) made a similar observation with post-mortem brains. In this study we have demonstrated that the human prefrontal cortex departs from nonhuman primate allometric trends, suggesting that there may have been selection for increased gyrification in the prefrontal cortex throughout hominid evolution. As discussed in the results section, an argument can be made to exclude the squirel monkey data from the regression line in Figure 10(a) and (b). When this is done, the slope of the nonhuman regression line is altered so that the human departure from allometry is less pronounced. The 95% confidence interval around the observed prefrontal GI (1·93, 2·39) no longer excludes the value predicted by the regression line for a species of our brain size (1·95). The same is true of the seventh coronal slice. The 95% confidence interval around the observed GI (2·57, 2·89) does not exclude the value predicted by the regression line for a brain of human size (2·62). With increased sample size, we expect that these results would become significant. This supposition is strengthened by Zilles *et al.*'s (1988) study that also reported the human prefrontal cortex to be uniquely gyrified.

If one accepts that the human prefrontal cortex is more gyrified than expected for our brain size, what could be the significance of

this finding? If the hypothesis of Richman and colleagues (1975) is correct, one possibility is that hominid evolution involved selection for increased intracortical processing in the prefrontal cortex that caused the outer cortical layers to expand more than the inner ones, thereby producing a highly gyrified region of cortex. A unique evolutionary modification in the human prefrontal cortex is intriguing because this brain region is involved in many cognitive operations that are especially well-developed in humans, such as symbolic thinking, knowledge of appropriate social behavior, decision-making, planning to achieve goals, and working memory (Grafman, 1995; Damasio, 1996; Goldman-Rakic, 1995; Deacon, 1997).

Finally, the seventh coronal slice is also significantly more gyrified in humans than expected for our brain size. In the human brain, slice 7 typically cuts near the posterior limit of the sylvian fissure in the vicinity of Wernicke's area (see Figure 12). Our data suggest that hominid evolution may have involved selection for increased cortical folding in a region of the brain that includes an area known to be involved with the comprehension and production of language.

Limitations and assumptions of this study

All of our brain volume estimates were obtained from captive subjects. We do not know if captive rearing has an impact on brain anatomy, but one should be cautious in generalizing these results to primates living in the wild. Due to limited availability, we were only able to acquire data from five species of monkeys, one of which is an outlier in many respects (*Cebus apella*). Therefore, we must also be cautious in drawing conclusions for ''monkeys'' based on this limited sample.

Whole brain cerebral white matter volume estimates were obtained by calculating the volume for the left hemisphere and doubling it. Hence, we assume that left and right hemisphere volumes are similar. In addition, gyrification indices are only calculated for the left hemisphere and it is assumed that the two hemispheres have a similar degree of convolutedness. In tracing the area of the neocortex manually in order to compare these results with those obtained using our own method, the left and right hemispheres were traced separately to provide an estimate of the magnitude of asymmetry in these brains. The following chart gives the left and right hemisphere volumes obtained by manually tracing the human and capuchin monkey neocortexes.

Species	Left hemisphere	Right hemisphere
Human	320·29 cc	318·71 cc
Capuchin monkey	19·17 cc	20·03 cc

In the human brain, doubling the left hemisphere volume would overestimate total neocortical volume by 1·58 cc (0·25%). In the capuchin brain, doubling left hemisphere volume would underestimate total neocortical volume by 0·86 cc (2·2%). Based on these results, we feel confident that true species differences would swamp any effect introduced by doubling left hemisphere volumes to obtain whole brain volumes.

Monkeys and apes were scanned using different receiving coils (knee coil and head coil, respectively) and in different positions (prone and supine, respectively). In monkeys, we opted for the knee coil because its smaller diameter affords an advantage in signal to noise ratio. Ape heads are too large for the knee coil to be used. It is possible that using two different coils could introduce a nonrandom bias in our measurements (monkeys *vs.* apes). However, since most of our analyses involve comparisons of relative structure sizes within an individual brain, this should not be a problem. Prone

vs. supine positioning could also introduce a minor bias in our measurements. We opted for prone positioning in monkeys because it reduces the risk that they will aspirate. Apes were scanned in the supine position because it affords easier access to the cubital vein where the IV catheter is placed and because this position makes it easier to keep the arm stationary and resting on the gantry of the scanner. The brain probably settles due to gravity and this could differentially influence gyrification measures in monkeys and apes due to their different positions. However, we did not observe any pronounced differences between monkeys and apes in their patterns of gyrification across the brain.

In future studies like this, it will be desirable to try to reduce or eliminate gradients in signal intensity across the brain to make gray–white segmentation more straightforward. We found that gradients were less pronounced when we were able to position the subject's head in the center of the receiving coil. Obviously, the human knee coil is designed to accommodate the human knee and not the head of the monkey. The monkey's short neck and wide shoulders sometimes prevented us from positioning the head as far into the knee coil as would be desirable. Consequently, the caudal portion of the brain is sometimes situated at or just outside the edge of the coil, where the signal begins to fade. This results in a more pronounced gradient in signal intensity. One solution to this problem would be to design coils specifically for monkeys and apes that better accommodate their anatomy and allow their heads to be positioned in the center of the coil. Alternatively, postprocessing steps can be used to correct for signal intensity gradients after the scan has been acquired (Wicks *et al.*, 1993; DeCarli *et al.*, 1996; Hertz *et al.*, 1998; Velthuizen *et al.*, 1998). In one approach a phantom of some homogenous material (e.g., water) is scanned to obtain a map of the strength of the reception field of the coil at each point, and this data is used to eliminate the gradient in the brain scan. This method demands that the coil be positioned consistently within the bore of the magnet on every scan. In practice, this is easy to ensure; however, the need to correct gradients must be anticipated in advance of collecting the scans, as was not the case in this study.

Finally, male and female data are pooled for each species. This procedure could obscure any sex differences that might exist in relative structure size. When relative brain size was analyzed separately for males and females, conclusions differed minimally from when the data were pooled. The statistical power afforded by pooling the data makes this a desirable approach.

Conclusions

All three hypotheses were supported by our analysis. The human neocortex is significantly larger than expected for a nonhuman primate of the same brain volume, the human prefrontal cortex is more gyrified than expected for a primate of our brain size, and neocortical gray matter volume does not keep pace with increases in cerebral white matter volume among anthropoid primates. These findings provide additional insights into human brain evolution beyond the important observation that brain volume approximately tripled in the hominid lineage (Tobias, 1971, 1995; Holloway, 1973, 1995). Our data suggest that hominid evolution involved extra-allometric expansion of the neocortex, a larger than expected increase in gyrification of the prefrontal and parietal/posterior temporal cortex, and an allometrically predictable increase in the ratio of neocortical connections to neocortical neuron number. These modifications may constitute part of the neurobiological substrate that supports some of our species most distinctive cognitive abilities (e.g., language, social intelligence).

Summary

In this paper we present results from the first comparative study of primate neuroanatomy to obtain data from living subjects with magnetic resonance imaging. We tested the following three hypotheses: (1) that the human neocortex is larger than expected for a primate of our brain size; (2) that the human prefrontal cortex is more convoluted than expected for a primate of our brain size; (3) that increases in cerebral white matter volume outpace increases in neocortical gray matter volume among anthropoid primates. Additionally, we conducted an analysis of relative brain size across our sample.

With respect to relative brain size among anthropoid primates, we confirm several conclusions that were reached through analysis of the post-mortem data set of Stephan and colleagues (1988). These include: (1) increases in brain size do not keep pace with increases in body size; (2) the human brain is significantly and dramatically larger than expected for an anthropoid primate of our body size; (3) great apes typically have larger brains for their body size than monkeys; and (4) capuchin monkeys are more encephalized than other monkey species. Our study has also produced several new insights with respect to relative brain size among anthropoids. Capuchins have a larger cross-sectional spinal cord area than expected for a primate of their body size. It is possible that the enlarged spinal cord area conveys a greater number of sensorimotor fibers to support this species' highly developed manual dexterity. In contrast, bonobos have small spinal cords for their body size and, consequently large brains for their spinal cord area. Finally, gorillas appear to depart from pongid allometric trends in having larger bodies than expected for their brain size which might reflect an evolutionary history of selection for increased body size.

To test the first of the three hypotheses, neocortical volume was regressed on the volume of the rest of the brain. This analysis revealed that the human neocortex (gray matter, white matter or gray plus white matter) is significantly larger than predicted by the nonhuman anthropoid regression line, suggesting that hominid evolution involved direct, specific selection for neocortical expansion, rather than selection for a global increase in brain size that followed nonhuman primate allometric trajectories and that acted uniformly on all brain structures. Thus, the first hypothesis is supported by our analysis.

Our analysis of gyrification confirmed the observation that larger anthropoid brains are more convoluted than smaller anthropoid brains, probably in order to accommodate an expanding neocortical surface that must fit within the confines of a spherically shaped skull. Capuchin brains are significantly less gyrified than expected for their size. Most of the 11 species follow a pattern of gyrification that involves increases in cortical folding (moving caudally from the rostral pole) that peak in the posterior parietal and anterior occipital lobe and then decline towards the occipital pole. To test the second of the three hypotheses, the gyrification index of the first coronal slice through the prefrontal cortex was regressed on brain volume. This analysis showed the human prefrontal cortex to be significantly more gyrified than expected for a nonhuman anthropoid of the same brain size. Thus, the second hypothesis is supported by our analysis. The human brain is also more gyrified than expected in a region of the brain that includes Wernicke's area. According to one explanation of cortical folding, this disproportionate gyrification would reflect selection for increased intracortical processing in these two areas of the human brain.

To test the third hypothesis, cerebral white matter volume was regressed against neocortical gray matter volume. This

analysis revealed that cerebral white matter scales at a higher power of brain volume than neocortical gray matter, suggesting that the number of axonal connections between neocortical neurons may increase faster than the number of neurons as brain size increases among anthropoid primates. Thus, larger brains are likely to have more connections relative to the number of neurons. However, the number of connections probably does not increase enough to maintain the same overall level of connectivity among neurons as brain size increases.

Acknowledgements

We are grateful to Brent Swenson, D.V.M. for his technical support. This work was supported in part by a grant from the L. S. B. Leakey Foundation and by the Yerkes Regional Primate Research Center grant NIH P51RR-00165.

References

Armstrong, E. (1985). Relative brain size in monkeys and prosimians. *Am. J. phys. Anthrop.* **66,** 263–273.

Barton, R. A. (1996). Neocortex size and behavioral ecology in primates. *Proc. R. Soc. Lond. series B* **263,** 173–177.

Beck, B. (1980). *Animal Tool Behavior: The Use and Manufacture of Tools by Animals*. New York: Garland.

Bonin, G. v. (1941*a*). On encephalometry: a preliminary study of the brain of man, chimpanzee, and macaque. *J. comp. Neurol.* **75,** 287–314.

Bonin, G. v. (1941*b*). Side lights on cerebral evolution: brain size of lower vertebrates and degree of cortical folding. *J. gen. Psychol.* **25,** 273–282.

Bonin, G. v. (1963). *The Evolution of the Human Brain*. Chicago: University of Chicago Press.

Clutton-Brock, T. H. & Harvey, P. H. (1980). Primates, brains and ecology. *J. Zool. Lond.* **190,** 309–323.

Damasio, A. R. (1996). The somatic marker hypothesis and the possible functions of the prefrontal cortex. *Phil. Trans. R. Soc. Lond. B* **351,** 1413–1420.

Deacon, T. W. (1988). Human brain evolution: II. Embryology and brain allometry. In (H. J. Jerison & I. Jerison, Eds) *Intelligence and Evolutionary Biology*, pp. 383–416. New York: Springer-Verlag.

Deacon, T. W. (1990). Rethinking mammalian brain evolution. *Am. Zool.* **30,** 629–705.

Deacon, T. W. (1997). *The Symbolic Species*. New York: W. W. Norton.

DeCarli, C., Murphy, D. G., Teichberg, D., Campbell, G. & Sobering, G. S. (1996). Local histogram correction of MRI spatially dependent image pixel intensity nonuniformity. *J. Magnetic Resonance Imag.* **6(3),** 519–528.

Elias, H. & Schwartz, D. (1971). Cerebro-cortical surface areas, volumes, lengths of gyri and their interdependence in mammals, including man. *Z. f. Saugetierkunde* **36,** 147–163.

Essen, D. C. V. (1997). A tension-based theory of morphogenesis and compact wiring in the central nervous system. *Nature* **285,** 313–318.

Falk, D. (1980). Hominid brain evolution: the approach from paleoneurology. *Yearb. phys. Anthrop.* **23,** 93–107.

Fragaszy, D. M. & Adams-Curtis, L. E. (1991). Generative aspects of manipulation in tufted capuchin monkeys (*Cebus apella*). *J. Comp. Psychol.* **105,** 387–397.

Frahm, H. D., Stephan, H. & Stephan, M. (1982). Comparison of brain structure volumes in insectivora and primates. I. Neocortex. *J. Hirnforsch.* **23,** 375–389.

Goldman-Rakic, P. (1995). Architecture of the prefrontal cortex and the central executive. *Ann. N.Y. Acad. Sci.* **769,** 71–83.

Grafman, J. (1995). Similarities and distinctions among current models of prefrontal cortical functions. *Ann. N.Y. Acad. Sci.* **769,** 337–368.

Harvey, P. H., Martin, R. D. & Clutton-Brock, T. H. (1987). Life histories in comparative perspective. In (B. Smuts, D. L. Cheney, R. M. Seyfarth, R. W. Wrangham & T. T. Struhsaker, Eds) *Primate Societies*, pp. 181–196. Chicago: University of Chicago Press.

Hemmer, H. (1966). Allometrische Untersuchungen am Schadel von *Homo sapiens* unter besonderer Berucksichtigung des Brachykephalisations-Problems. *Homo* **17,** 190–209.

Hertz, L., Brummer, M. & Faber, T. (1997). Improvements in gray/white matter segmentation with RF uniformity correction. 5th Scientific Meeting of the ISMRM.

Hofman, M. A. (1989). On the evolution and geometry of the brain in mammals. *Progress in Neurobiology* **32,** 137–158.

Holloway, R. L. (1973). Endocranial volumes of early African hominids, and the role of the brain in human mosaic evolution. *J. hum. Evol.* **2,** 449–459.

Holloway, R. L. (1995). Toward a synthetic theory of human brain evolution. In (J.-P. Changeux & J. Chavaillon, Eds) *Origins of the Human Brain*, pp. 42–60. Oxford: Clarendon Press.

Holloway, R. L. & Shapiro, J. S. (1992). Relationship of squamosal suture to asterion in pongids (Pan): relevance to early hominid brain evolution. *Am. J. phys. Anthrop.* **89,** 275–282.

Jerison, H. J. (1973). *Evolution of the Brain and Intelligence*. New York: Academic Press.

Jerison, H. J. (1982). Allometry, brain size, cortical surface, and convolutedness. In (E. Armstrong &

D. Falk, Eds) *Primate Brain Evolution*, pp. 77–84. New York: Plenum Press.

Kretschmann, H. J., Tafesse, U. & Herrmann, A. (1982). Different volume changes of cerebral cortex and white matter during histological preparation. *Microscop. Acta* **86,** 13–24.

Martin, R. D. (1973). Comparative anatomy and primate systematics. *Symp. zool. Soc. Lond.* **33,** 301–337.

Parker, S. T. & Gibson, K. R. (1977). Object manipulation, tool use, and sensorimotor intelligence in Cebus monkeys and great apes. *J. hum. Evol.* **6,** 623–641.

Passingham, R. (1982). *The Human Primate*. San Francisco: W. H. Freeman.

Passingham, R. E. (1973). Anatomical differences between the neocortex of man and other primates. *Brain, Behavior, and Evolution* **7,** 337–359.

Passingham, R. E. & Ettlinger, G. (1974). A comparison of cortical functions in man and the other primates. *International Review of Neurobiology* **16,** 233–299.

Pilbeam, D. & Gould, S. J. (1974). Size and scaling in human evolution. *Science* **186,** 892–901.

Radinsky, L. (1972). Endocasts and studies of primate brain evolution. In (R. Tuttle, Ed.) *The Functional and Evolutionary Biology of Primates*. Chicago: Aldine-Atherton.

Radinsky, L. (1975). Primate brain evolution. *Am. Scient.* **63,** 656–663.

Richman, D., Stewart, R., Hutchinson, J. *et al.* (1975). Mechanical model of brain convolutional development. *Science* **189,** 18–21.

Rowe, N. (1996). *The Pictorial Guide to the Living Primates*. East Hampton: Pogonias Press.

Smith, G. E. (1902). On the morphology of the brain in the Mammalia, with special reference to that of the lemurs, recent and extinct. *Trans. Linn. Soc., Lond. (Zool.)* **8,** 319–432.

Stephan, H. & Andy, O. J. (1969). Quantitative comparative neuroanatomy of primates: an attempt at a phylogenetic interpretation. *Ann. N.Y. Acad. Sci.* **167,** 370–387.

Stephan, H., Baron, G. & Frahm, H. D. (1988). Comparative size of brain and brain components. *Comp. Primate Biol.* **4,** 1–38.

Stephan, H., Bauchot, R. & Andy, O. (1970). Data on size of the brain and of various brain parts in insectivores and primates. In (M. Noback, Ed.) *The Primate Brain. Advances in Primatology*, pp. 289–297. New York: Appleton Century Crofts.

Stephan, H., Frahm, H. & Baron, G. (1981). New and revised data on volumes of brain structures in insectivores and primates. *Folia primatol.* **35,** 1–29.

Tanner, J. M. (1990). *Fetus into Man*. Cambridge, MA: Harvard University Press.

Tobias, P. V. (1971). *The Brain in Hominid Evolution*. New York: Columbia University Press.

Tobias, P. V. (1995). The brain of the first hominids. In (J.-P. Changeux & J. Chavillon, Eds) *Origins of the Human Brain*, pp. 61–81. Oxford: Clarendon Press.

Visalberghi, E. (1990). Tool use in *Cebus*. *Folia primatol.* **54,** 146–154.

Velthuizen, R. P., Heine, J. J., Cantor, A. B., Lin, H., Fletcher, L. M. & Clarke, L. P. (1998). Review and evaluation of MRI nonuniformity corrections for brain tumor response measurements. *Medical Physics* **25(9),** 1655–1666.

Westergaard, G. C. (1994). The subsistence technology of capuchins. *Int. J. Primatol.* **15,** 899–906.

Wicks, D. A., Barker, G. J. & Tofts, P. S. (1993). Correction of intensity nonuniformity in MR images of any orientation. *Magnetic Resonance Imaging* **11(2),** 183–196.

Zilles, K., Armstrong, E., Moser, K. H., Schleicher, A. & Stephan, H. (1989). Gyrification in the cerebral cortex of primates. *Brain Behav. Evol.* **34,** 143–150.

Zilles, K., Armstrong, E., Schleicher, A. & Kretschmann, H.-J. (1988). The human pattern of gyrification in the cerebral cortex. *Anatomy and Embryology* **179,** 173–179.